

GSA Data Repository Item 2018082

Behrensmeyer, A.K., Potts, R., and Deino, A., 2018, The Oltulelei Formation of the southern Kenyan Rift Valley: A chronicle of rapid landscape transformation over the last 500 k.y.: Geological Society of America Bulletin, <https://doi.org/10.1130/B31853.1>.

DATA REPOSITORY

SUPPLEMENTAL FILES

DR1. Deino dating - $^{40}\text{Ar}/^{39}\text{Ar}$ Methods

DR2. Oltulelei Fm. lithofacies and inferred depositional environments

DR3. Detailed description of Oltulelei Fm. Members and reference panels for Oltulelei Fm. stratigraphy.

A. Locality B

B. Locality OLT

C. Locality G

Link location: http://www.geosociety.org/datarerepository/2018/2018xxx_Tables.xls

SUPPLEMENTAL TEXT DR1

$^{40}\text{Ar}/^{39}\text{Ar}$ Methods

All radioisotopic ages reported in this manuscript were obtained by the $^{40}\text{Ar}/^{39}\text{Ar}$ dating method, applied to individual K-feldspar phenocrysts separated from tuffaceous samples collected from outcrop exposures in the Olorgesailie field area. Some of these ages were initially published in Deino and Potts (1990), and herein revised for re-calibrations of the argon dating standard and decay constants (Kuiper et al., 2008; Niespolo et al., 2016). In addition, dating results of nine new samples are reported, collected during field studies in 2001, 2004, 2005, 2010, and 2011. Text Table 1 provides location data and a brief description of each new sample.

Feldspar phenocryst separates were obtained from these samples by standard mineral separation techniques., incorporating a brief final stage of dilute HF treatment and hand-picking to minimize inclusions. The separates were irradiated in the CLICIT position of the Oregon State University TRIGA reactor in five batches. One irradiation (#290, Table DR1-1) employed sanidine from the Fish Canyon Tuff of Colorado as a monitor mineral (orbitally tuned age of 28.201 ± 0.023 1σ Ma; Kuiper et al., 2008), whereas all others used sanidine phenocrysts from the Alder Creek Rhyolite of California (age = 1.1848 ± 0.006 Ma; Niespolo et al., 2016). Irradiation 413 was irradiated for 0.07 h; 290 for 0.25 h; 359 for 0.5 h; and 326 and 329 for 1 h (Tables DR1-1 and –3). Reactor-induced isotopic production ratios for these irradiations were: $(^{36}\text{Ar}/^{37}\text{Ar})_{\text{Ca}} = 2.65 \pm 0.02 \times 10^{-4}$, $(^{38}\text{Ar}/^{37}\text{Ar})_{\text{Ca}} = 1.96 \pm 0.08 \times 10^{-5}$, $(^{39}\text{Ar}/^{37}\text{Ar})_{\text{Ca}} = 6.95 \pm 0.09 \times 10^{-4}$, $(^{37}\text{Ar}/^{39}\text{Ar})_{\text{K}} = 2.24 \pm 0.16 \times 10^{-4}$, $(^{38}\text{Ar}/^{39}\text{Ar})_{\text{K}} = 1.220 \pm 0.003 \times 10^{-2}$, $(^{40}\text{Ar}/^{39}\text{Ar})_{\text{K}} = 2.5 \pm 0.9 \times 10^{-4}$. Atmospheric $^{40}\text{Ar}/^{36}\text{Ar} = 298.56 \pm 0.31$ (Lee et al., 2006) and decay constants were according to Min et al. (2000).

Following a period of at least several weeks of radiological ‘cooling’ after irradiation, the feldspars were analyzed individually by the $^{40}\text{Ar}/^{39}\text{Ar}$ method using two laser-heating methods,

single-crystal total fusion (SCTF) and single-crystal incremental heating (SCIH). In the SCTF technique, individual feldspar phenocrysts are exposed to a diffuse laser beam at low power to drive off surficial gasses, then fused and analyzed with a focused beam in a single step. These SCTF analyses were performed on an older generation of mass spectrometer, a MAP 215 instrument. In the SCIF technique, individual phenocrysts were incrementally heated in 5–10 steps at progressively increasing power to fusion, to better examine the argon systematics of the grain and more effectively drive off atmospheric contamination. These detailed analyses were conducted on a newer, more sensitive mass spectrometer utilizing a high-efficiency ionization source, simultaneous multi-isotope measurement, and all ion-counting detectors (a Nu Instruments *Noblesse* noble-gas mass spectrometer). Further details of the analytical technique can be found in Deino et al. (2010) and Niespolo et al. (2016).

$^{40}\text{Ar}/^{39}\text{Ar}$ Results

Age-probability density spectra of the SCTF dating results are shown in Figure DR1-1, and full analytical data are provided in Table DR1-1. Several samples exhibit outliers much older than the inferred stratigraphic age, and these grains are interpreted as xenocrysts incorporated during transportation and deposition. In addition, skewness toward older ages is evident in one of the samples (OL04/B-WS6a). To mitigate the effect of xenocrystic grains, older tails, and analytical outliers, a robust outlier detection scheme has been applied based on the nMAD statistic ('normalized median absolute deviation') where grains with ages >2 nMad from the median are considered outliers and eliminated. Following outlier elimination, each of the seven samples is characterized by a strongly dominant mode near the youngest edge of the age distribution, interpreted as the juvenile volcanic eruptive age. We note that there are a few grains younger than the inferred juvenile mode at 223 ka in sample OL04/B-WS6a; the origin of these grains is uncertain, and may be contaminants introduced geologically by bioturbation or during sample processing, but overall geological relationships suggest that the dominant mode provides a geologically reasonable eruption age. Isochron correlation analysis of the juvenile mode data yield the final set of ages for these samples (Figure DR1-2, Table DR1-2). The isochron ages are preferred over the direct analytical calculation of individual ages since the isochron approach makes no a priori assumption about the trapped $^{40}\text{Ar}/^{36}\text{Ar}$ composition of the grains (i.e., does not assume an atmospheric ratio).

Incremental-heating spectra for the SCIH experiments are shown in Figure DR1-3, and analytical data provided in Table DR1-3. Most grains yielded apparent-age plateaus. The 'age plateau' identification algorithm used here identifies the set of contiguous steps encompassing the greatest percent of ^{39}Ar release that exhibit an acceptable MSWD ('mean square of weighted deviates,' with a threshold probability $>95\%$ that the observed scatter is due to analytical error alone and that geological scatter is not demonstrated). A plateau must comprise at least 50% of the total ^{39}Ar release and consist of at least three consecutive steps. The plateau ages shown in Figure DR1-3 are thus isochron ages. The isochrons themselves, using the plateau subsets, are shown in Figure DR1-4 and Table DR1-4, while the probability-density spectra of the isochron results in given in Figure DR1-5. Sample OL11/OLT-1, pumice clasts deposited in a stratigraphic setting, shows a simple unimodal distribution with a single outlier, and a readily interpreted eruptive age. Sample OL10/BOK2-4b, however, requires a different interpretation: it is derived from pumice in a near-vertical clastic dike emplaced in early Olkesiteti (OK) Mbr deposits in Locality B. Though the host stratigraphy of the dike is ~ 300 ka, pumice in the dike

yield ages from ~2 Ma to 200 ka. The dike was likely emplaced sometime after the eruption age of the youngest components at 200 ± 11 ka.

REFERENCES CITED

- Deino, A., and Potts, R., 1990, Single-crystal $40\text{Ar}/39\text{Ar}$ dating of the Olorgesailie Formation, Southern Kenya Rift: *Journal of Geophysical Research*, v. 95, B6, p. 8453–8470, <https://doi.org/10.1029/JB095iB06p08453>.
- Deino, A., and Potts, R., 1992, Age-Probability Spectra for Examination of Single-Crystal $40\text{Ar}/39\text{Ar}$ Dating Results: Examples from Olorgesailie, Southern Kenya Rift: *Quaternary International*, v. 7/8, p. 81–89.
- Deino, A.L., Scott, G., Saylor, B., Mulugeta, A., Angelini, J.D., and Haile-Selassie, Y., 2010, $^{40}\text{Ar}/^{39}\text{Ar}$ dating, paleomagnetism, and tephrochemistry of Pliocene strata of the hominid-bearing Woranso-Mille area, west-central Afar Rift, Ethiopia: *Journal of Human Evolution*, v. 58, p. 111–126, <https://doi.org/10.1016/j.jhevol.2009.11.001>.
- Kuiper, K.F., Deino, A., Hilgen, F.J., Krijgsman, W., Renne, P.R., and Wijbrans, J.R., 2008, Synchronizing Rock Clocks of Earth History: *Science*, v. 320, no. 5875, p. 500–504, <https://doi.org/10.1126/science.1154339>.
- Lee, J.-Y., Marti, K., Severinghaus, J.P., Kawamura, K., Yoo, H.-S., Lee, J.B., and Kim, J.S., 2006, A redetermination of the isotopic abundances of atmospheric Ar: *Geochimica et Cosmochimica Acta*, v. 70, p. 4507–4512, <https://doi.org/10.1016/j.gca.2006.06.1563>.
- Min, K.W., Mundil, R., Renne, P.R., and Ludwig, K.R., 2000, A test for systematic errors in Ar-40/Ar-39 geochronology through comparison with U/Pb analysis of a 1.1-Ga rhyolite: *Geochimica et Cosmochimica Acta*, v. 64, no. 1, p. 73–98, [https://doi.org/10.1016/S0016-7037\(99\)00204-5](https://doi.org/10.1016/S0016-7037(99)00204-5).
- Niespolo, E.M., Rutte, D., Deino, A.L., and Renne, P.R., 2016, Intercalibration and age of the Alder Creek sanidine $^{40}\text{Ar}/^{39}\text{Ar}$ standard: *Quaternary Geochronology*, [10.1016/j.quageo.2016.09.004](https://doi.org/10.1016/j.quageo.2016.09.004).

FIGURE CAPTIONS

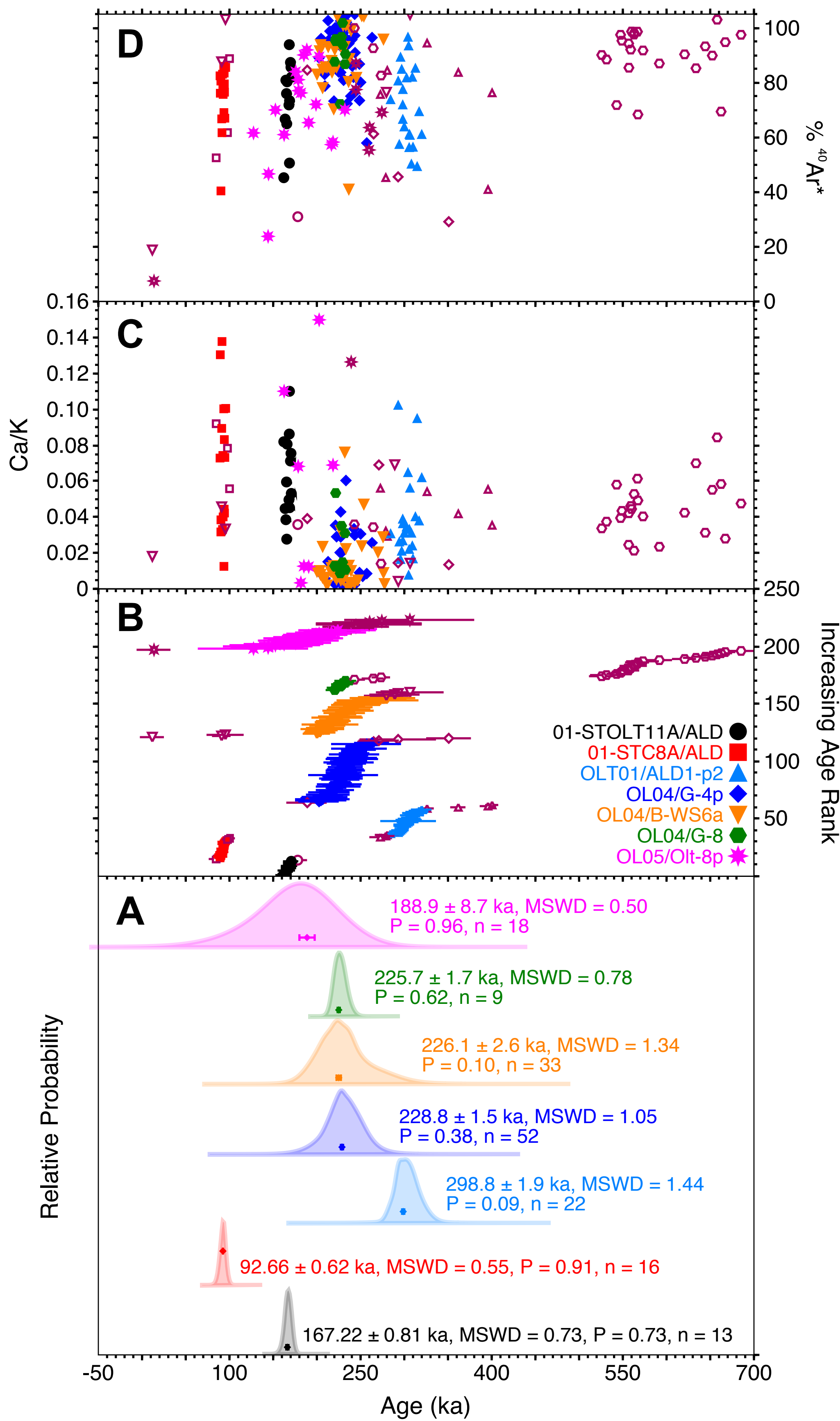
Figure DR1-1. **(A)** Age-probability density spectra of SCTF analyses. The vertical scale is a relative probability measure that expresses the likelihood of a given age occurring in the sample, obtained by summing the unit gaussian age probabilities of individual analyses (Deino and Potts, 1992). Weighted-mean ages of the juvenile population are shown with the total (internal and external) 1σ analytical error. ‘MSWD’ refers to ‘mean square of weighted deviates,’ a measure of the observed scatter about the fit line, compared to the expected scatter. ‘P’ refers to the probability that the observed scatter can be explained by analytical errors alone; a value below 0.05 in this circumstance would indicate that analytical errors are insufficient to explain the magnitude of the dispersion (i.e., geological scatter is present). ‘n’ is the included number of analyses. **(B)** Individual analyses with 1σ analytical uncertainty, sorted vertically by increasing age on a sample-by-sample basis. Closed symbols in the upper plots represent analyses included in the mean, whereas open symbols represent excluded grains. **(C)** The weighted-mean atomic Ca/K ratio. **(D)** Percent radiogenic ($^{40}\text{Ar}^*$) yield.

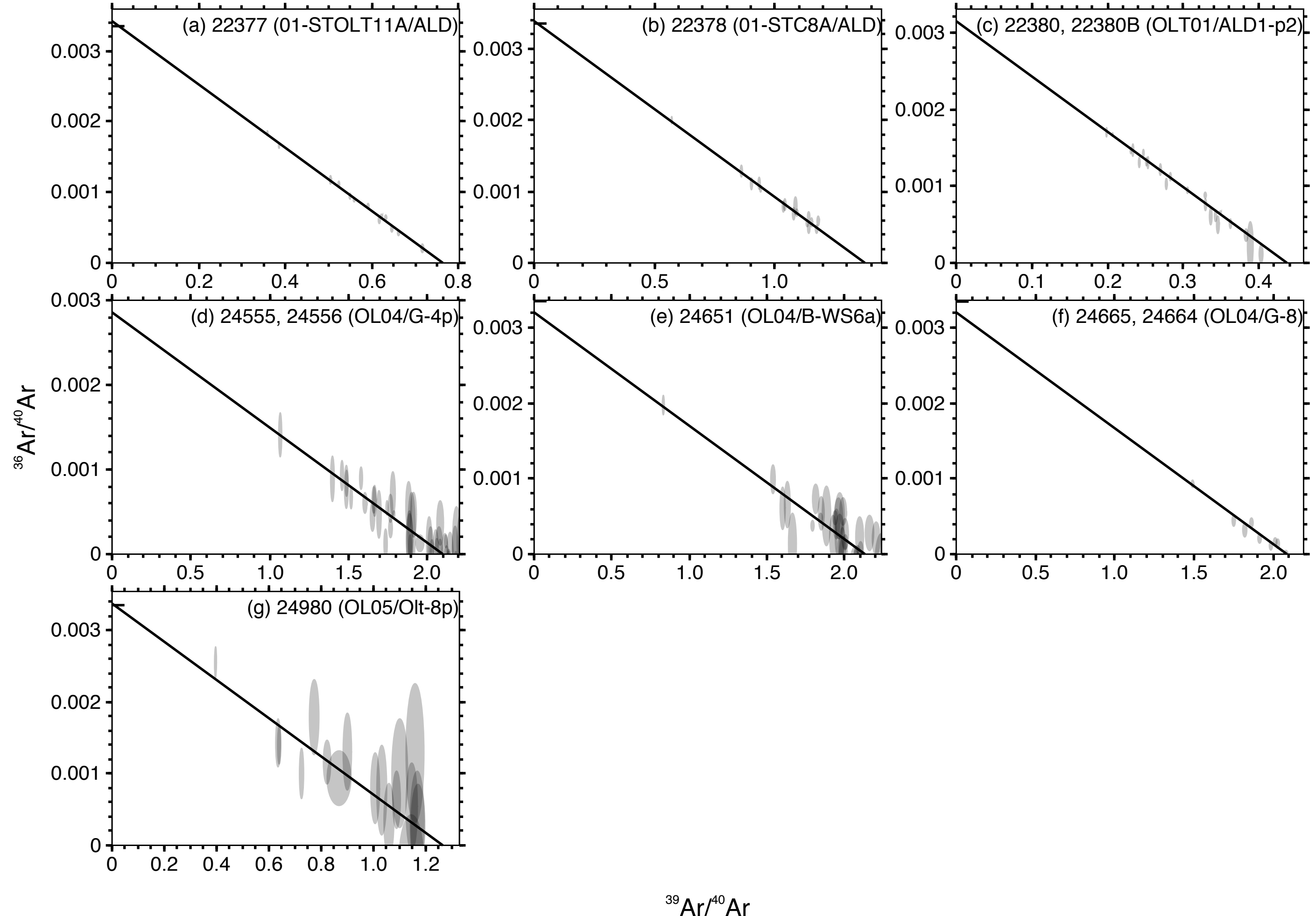
Figure DR1-2. ‘Inverse’ isochron plots ($^{36}\text{Ar}/^{40}\text{Ar}$ versus $^{39}\text{Ar}/^{40}\text{Ar}$ isotope correlation diagrams) of inferred juvenile analyses from the SCTF experiments. The age is derived from the x -axis intercept. ‘ $^{40}\text{Ar}/^{39}\text{Ar}$ Int.’ refers to ‘trapped’ non-radiogenic $^{40}\text{Ar}/^{36}\text{Ar}$ ratio derived from y -axis intercept of the isochron.

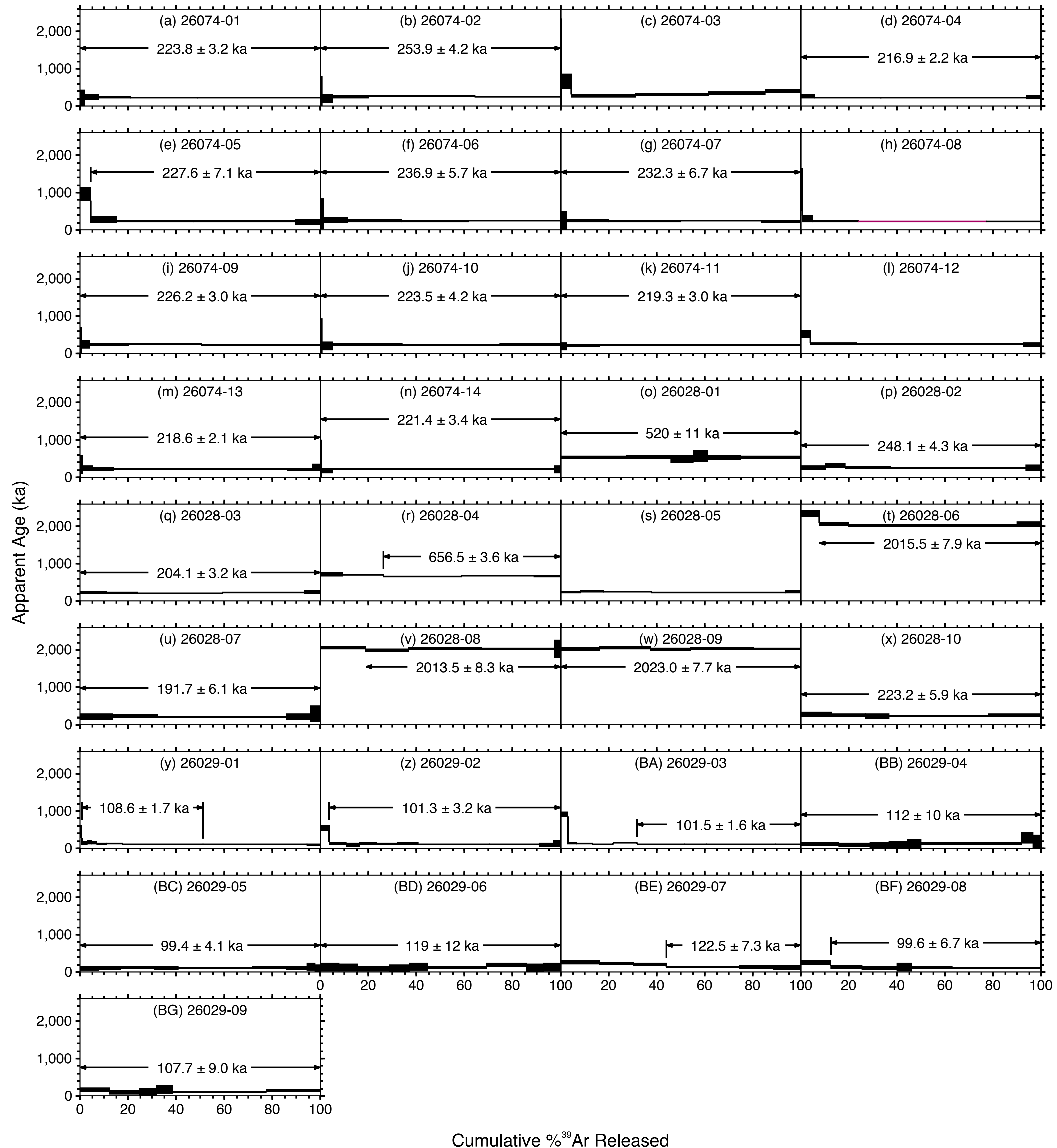
Figure DR1-3. Incremental heating release spectra from the SCIH experiments, plotted on a grain-by-grain basis, showing apparent age plotted against the percent ^{39}Ar release for each step. Individual plots are titled by laboratory run ID in parenthesis.

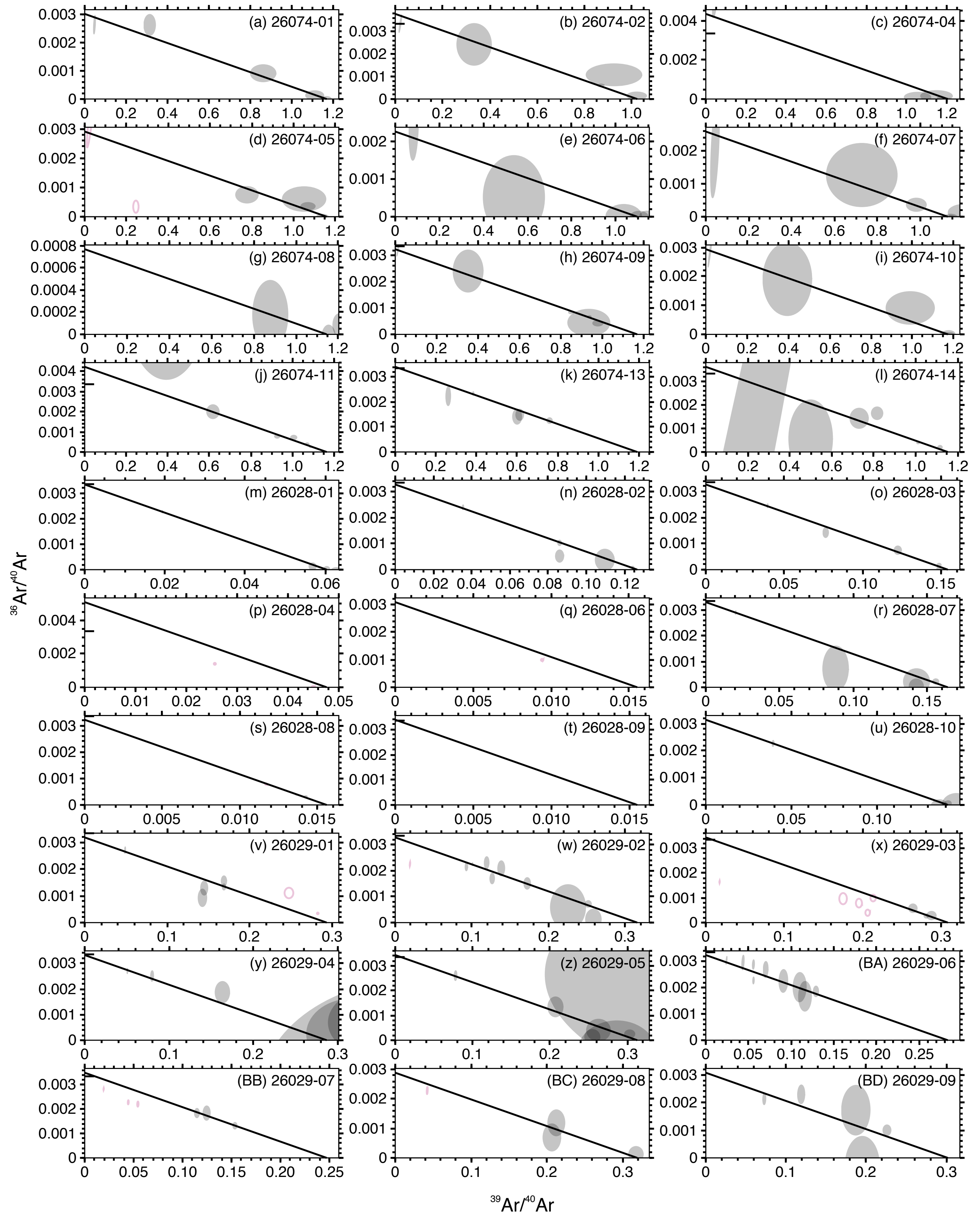
Figure DR1-4. Inverse-isochron plots of plateau steps from incremental heating experiments. Each grain is plotted separately.

Figure DR1-5. Age-probability density plot of ages derived from isochron analysis.









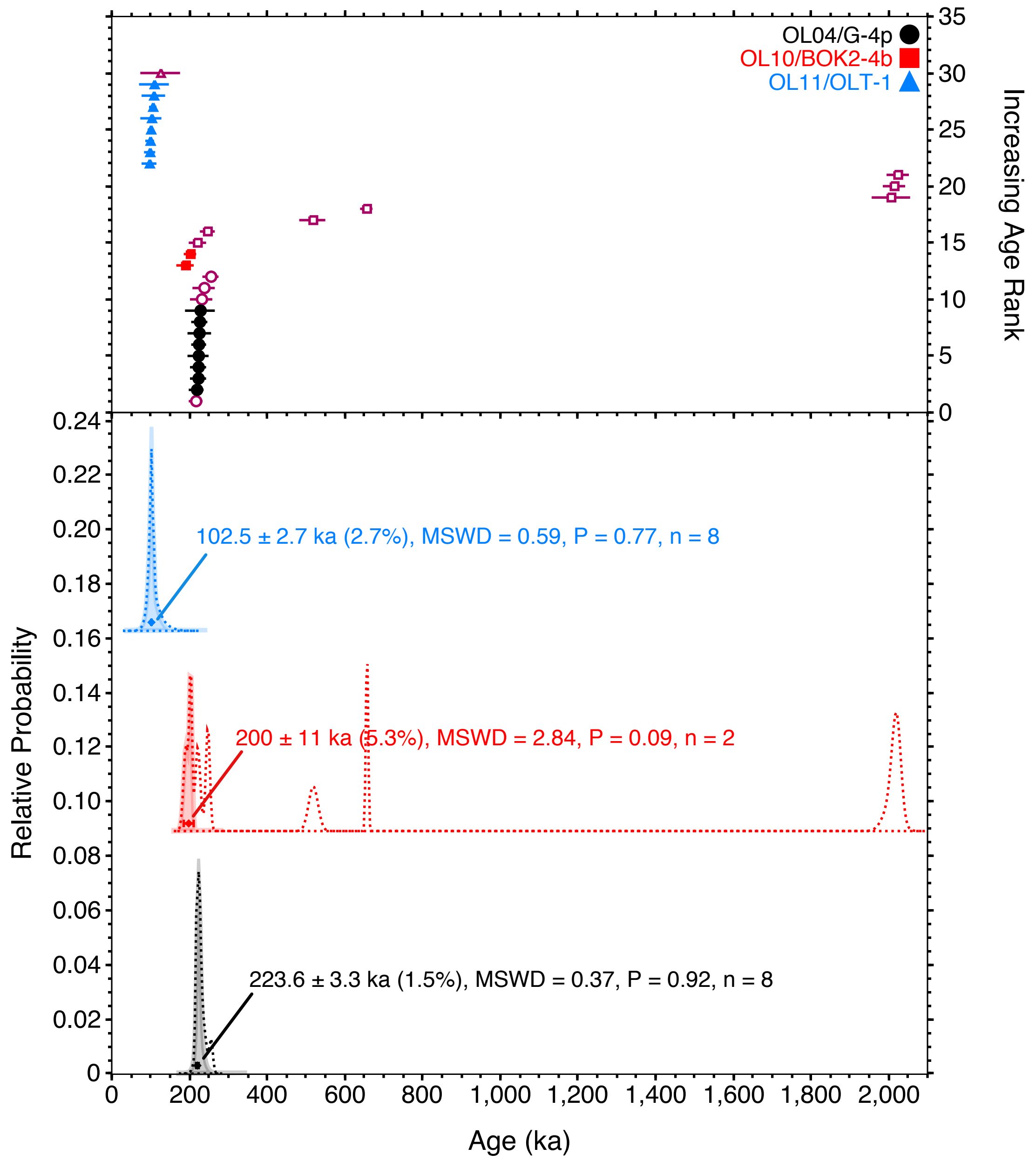


TABLE DR-1 - SCTF analytical data

Lab ID#	Watts Irrad.	J (X 10 ⁻³) ± 1σ	Relative Isotopic Abundances					Derived Results					Inverse Isochron Data													
			⁴⁰ Ar ±1σ	³⁹ Ar ±1σ	³⁸ Ar ±1σ	³⁷ Ar ±1σ	³⁶ Ar ±1σ	³⁹ Ar Mol ∞ 10 ⁻¹⁵	Ca/K ±1σ	⁴⁰ Ar / ³⁹ Ar ±1σ	% ⁴⁰ Ar ±1σ	Age (Ma) ±1σ	³⁶ Ar / ⁴⁰ Ar ±%1σ	³⁹ Ar / ⁴⁰ Ar ±%1σ	³⁶ Ar / ³⁹ Ar Er. Corr.											
<i>01-STOLT11A/ALD</i>																										
22377-01	9.0	290A	0.07020	0.00011	0.312136	0.000757	0.201340	0.000337	0.002546	0.000052	0.002601	0.000063	0.000153	0.000015	1.26	0.0754	0.0020	1.3256 ± 0.0232	85.6	170.4	3.0	0.00048	9.88	0.64558	0.41	0.0948
22377-02	8.0	290A	0.07020	0.00011	0.458001	0.000831	0.176385	0.000271	0.002377	0.000039	0.003289	0.000073	0.000761	0.000016	1.10	0.1100	0.0026	1.3121 ± 0.0323	50.6	168.6	4.1	0.00166	2.34	0.38537	0.37	0.3918
22377-03	8.0	290A	0.07020	0.00011	0.482774	0.000844	0.269511	0.000514	0.003233	0.000049	0.002063	0.000038	0.000432	0.000014	1.68	0.0452	0.0009	1.3129 ± 0.0185	73.4	168.7	2.4	0.00089	3.46	0.55869	0.38	0.2649
22377-04	8.0	290A	0.07020	0.00011	0.364663	0.000736	0.226465	0.000403	0.002764	0.000048	0.003084	0.000042	0.000244	0.000011	1.42	0.0806	0.0015	1.2912 ± 0.0161	80.2	165.9	2.1	0.00066	4.50	0.62153	0.39	0.2056
22377-05	8.0	290A	0.07020	0.00011	0.355489	0.000729	0.127310	0.000254	0.001734	0.000031	0.001760	0.000054	0.000654	0.000012	0.80	0.0819	0.0026	1.2616 ± 0.0350	45.2	162.2	4.5	0.00184	2.13	0.35835	0.40	0.4309
22377-06	7.0	290A	0.07020	0.00011	0.297602	0.000663	0.175660	0.000263	0.002178	0.000047	0.001763	0.000044	0.000241	0.000011	1.10	0.0595	0.0016	1.2857 ± 0.0209	75.9	165.2	2.7	0.00081	4.74	0.59073	0.39	0.1967
22377-07	7.0	290A	0.07020	0.00011	0.297227	0.000672	0.187554	0.000263	0.002291	0.000040	0.001217	0.000051	0.000192	0.000011	1.17	0.0385	0.0017	1.2802 ± 0.0194	80.8	164.5	2.5	0.00064	5.93	0.63155	0.39	0.1575
22377-08	7.0	290A	0.07020	0.00011	0.573852	0.000838	0.128125	0.000224	0.001821	0.000033	0.000772	0.000045	0.001327	0.000014	0.80	0.0358	0.0021	1.3861 ± 0.0508	31.0	178.1	6.5	0.00231	1.54	0.22339	0.36	0.5848
22377-09	7.0	290A	0.07020	0.00011	0.276904	0.000608	0.182886	0.000234	0.002180	0.000041	0.001289	0.000063	0.000119	0.000011	1.14	0.0712	0.0022	1.3210 ± 0.0191	87.3	169.8	2.5	0.00042	9.37	0.66103	0.38	0.0997
22377-10	7.0	290A	0.07020	0.00011	0.165334	0.000499	0.118272	0.000243	0.001490	0.000024	0.001712	0.000062	0.000036	0.000010	0.74	0.0862	0.0032	1.3103 ± 0.0266	93.8	168.4	3.4	0.00021	29.78	0.71599	0.47	0.0319
22377-11	7.0	290A	0.07020	0.00011	0.264238	0.000590	0.144984	0.000242	0.001861	0.000033	0.000107	0.000044	0.000250	0.000011	0.91	0.0496	0.0019	1.3076 ± 0.0254	71.8	168.1	3.3	0.00094	4.65	0.54912	0.40	0.2002
22377-12	7.0	290A	0.07020	0.00011	0.314651	0.000663	0.164531	0.000233	0.002073	0.000038	0.001231	0.000044	0.000353	0.000013	1.03	0.0447	0.0017	1.2734 ± 0.0257	66.6	163.7	3.3	0.00112	3.78	0.52330	0.38	0.2457
22377-13	7.0	290A	0.07020	0.00011	0.214938	0.000584	0.108253	0.000214	0.001391	0.000029	0.000501	0.000025	0.000253	0.000013	0.68	0.0277	0.0014	1.2878 ± 0.0378	64.9	165.5	4.9	0.00118	5.23	0.50403	0.44	0.1797
22377-14	7.0	290A	0.07020	0.00011	0.263491	0.000596	0.162343	0.000263	0.001983	0.000042	0.001441	0.000052	0.000161	0.000013	1.01	0.0531	0.0020	1.3284 ± 0.0252	81.9	170.7	3.2	0.00061	8.22	0.61663	0.40	0.1135
<i>01-STC8A/ALD</i>																										
22378-02	7.0	290A	0.06980	0.00011	0.167048	0.000514	0.172789	0.000313	0.002089	0.000028	0.001218	0.000058	0.000133	0.000013	1.08	0.0422	0.0020	0.7383 ± 0.0230	76.5	94.3	2.9	0.00079	9.89	1.03555	0.46	0.0964
22378-03	7.0	290A	0.06980	0.00011	0.153119	0.000520	0.138131	0.000253	0.001624	0.000037	0.001685	0.000056	0.000171	0.000013	0.86	0.0732	0.0025	0.7415 ± 0.0283	67.0	94.7	3.6	0.00111	7.55	0.90305	0.48	0.1275
22378-04	7.0	290A	0.06980	0.00011	0.144825	0.000503	0.150708	0.000262	0.001843	0.000038	0.001066	0.000046	0.000119	0.000012	0.94	0.0401	0.0019	0.7261 ± 0.0243	75.7	92.8	3.1	0.00082	10.14	1.04182	0.49	0.0953
22378-05	7.0	290A	0.06980	0.00011	0.125934	0.000471	0.142481	0.000302	0.001773	0.000035	0.001321	0.000042	0.000049	0.000012	0.89	0.0557	0.0019	0.7834 ± 0.0249	88.7	100.1	3.2	0.00038	24.59	1.13276	0.52	0.0396
22378-06	7.0	290A	0.06980	0.00011	0.137999	0.000502	0.148668	0.000202	0.001849	0.000028	0.002053	0.000054	0.000097	0.000012	0.93	0.0831	0.0023	0.7369 ± 0.0244	79.5	94.1	3.1	0.00069	12.53	1.07856	0.51	0.0774
22378-07	7.0	290A	0.06980	0.00011	0.246846	0.000583	0.279728	0.000482	0.003401	0.000053	0.002058	0.000060	0.000139	0.000012	1.75	0.0444	0.0014	0.7353 ± 0.0133	83.4	93.9	1.7	0.00056	8.65	1.13459	0.41	0.1080
22378-08	7.0	290A	0.06980	0.00011	0.169429	0.000480	0.199729	0.000323	0.002486	0.000044	0.002410	0.000062	0.000102	0.000011	1.25	0.0728	0.0020	0.6984 ± 0.0175	82.4	89.2	2.2	0.00059	11.42	1.18030	0.43	0.0830
22378-09	7.0	290A	0.06980	0.00011	0.157400	0.000462	0.179384	0.000313	0.002293	0.000046	0.002983	0.000071	0.000079	0.000012	1.12	0.1005	0.0026	0.7493 ± 0.0196	85.5	95.7	2.5	0.00049	15.07	1.14104	0.45	0.0631
22378-10	7.0	290A	0.06980	0.00011	0.181865	0.000498	0.209354	0.000402	0.002573	0.000052	0.001144	0.000050	0.000104	0.000011	1.31	0.0331	0.0015	0.7205 ± 0.0169	83.0	92.0	2.2	0.00057	11.11	1.15257	0.45	0.0847
22378-11	7.0	290A	0.06980	0.00011	0.191924	0.000500	0.224979	0.000461	0.002772	0.000039	0.003724	0.000065	0.000094	0.000011	1.41	0.1002	0.0020	0.7319 ± 0.0156	85.9	93.5	2.0	0.00047	12.51	1.17367	0.44	0.0750
22378-12	7.0	290A	0.06980	0.00011	0.240226	0.000552	0.225862	0.000402	0.002847	0.000042	0.000467	0.000035	0.000250	0.000011	1.41	0.1215	0.0025	0.7332 ± 0.0161	69.0	93.7	2.1	0.00104	4.63	0.94123	0.41	0.2011
22378-13	7.0	290A	0.06980	0.00011	0.221723	0.000555	0.178619	0.000233	0.002309	0.000049	0.002305	0.000058	0.000286	0.000011	1.12	0.0783	0.0021	0.7650 ± 0.0207	61.7	97.7	2.6	0.00128	4.17	0.80638	0.40	0.2255
22378-14	7.0	290A	0.06980	0.00011	0.214559	0.000534	0.233911	0.000412	0.002972	0.000044	0.002860	0.000061	0.000153	0.000011	1.46	0.0743	0.0017	0.7237 ± 0.0145	79.0	92.5	1.9	0.00070	7.19	1.09148	0.42	0.1303
22378-15	7.0	290A	0.06980	0.00011	0.140974	0.000445	0.111360	0.000243	0.001389	0.000032	0.001682	0.000056	0.000226	0.000011	0.70	0.0920	0.0032	0.6637 ± 0.0313	52.5	84.8	4.0	0.00159	5.10	0.79069	0.49	0.1871
22378-16	7.0	290A	0.06980	0.00011	0.153021	0.000443	0.174347	0.000312	0.002177	0.000040	0.000907	0.000043	0.000101	0.000010	1.09	0.0317	0.0015	0.7059 ± 0.0176	80.5	90.2	2.2	0.00065	9.98	1.14076	0.45	0.0950
22378-17	7.0	290A	0.06980	0.00011	0.217089	0.000585	0.124012	0.000194	0.001568	0.000038	0.000781	0.000042	0.000434	0.000011	0.78	0.0384	0.0021	0.7064 ± 0.0298	40.4	90.2	3.8	0.00200	2.75	0.57171	0.42	0.3422
22378-18	7.0	290A	0.06980	0.00011	0.122336	0.000426	0.114267	0.000233	0.001434	0.000035	0.001672	0.000054	0.000138	0.000010	0.71	0.0893	0.0030	0.7134 ± 0.0276	66.7	91.1	3.5	0.00112	7.58	0.93503	0.50	0.1272
22378-19	7.0	290A</td																								

TABLE DR-1 - SCTF analytical data

Lab ID#	Watts Irrad.	J (X 10 ⁻³) ± 1σ	Relative Isotopic Abundances										Derived Results								Inverse Isochron Data							
			⁴⁰ Ar		³⁹ Ar		³⁸ Ar		³⁷ Ar		³⁶ Ar		³⁹ Ar Mol		Ca/K		⁴⁰ Ar / ³⁹ Ar		% ⁴⁰ Ar		Age (Ma)		³⁶ Ar / ⁴⁰ Ar		³⁹ Ar / ⁴⁰ Ar		³⁶ Ar / ³⁹ Ar	
			±1σ	±1σ	±1σ	±1σ	±1σ	±1σ	±1σ	±1σ	±1σ	±1σ	∞ 10 ⁻¹⁵	±1σ	±1σ	±1σ	±1σ	±1σ	±1σ	±1σ	±1σ	±1σ	Er. Corr.					
22380B-05	7.0	290A	0.06930	0.00011	0.159797	0.000414	0.040439	0.000115	0.000475	0.000026	0.000203	0.000026	0.000209	0.000013	0.25	0.0331	0.0043	2.4100	± 0.0948	61.0	305.8	12.0	0.00131	6.06	0.25322	0.44	0.1108	
22380B-06	7.0	290A	0.06930	0.00011	0.127001	0.000398	0.029609	0.000104	0.000412	0.000020	0.000098	0.000028	0.000186	0.000010	0.19	0.0219	0.0062	2.4084	± 0.1059	56.2	305.6	13.4	0.00147	5.54	0.23328	0.52	0.1227	
22380B-07	7.0	290A	0.06930	0.00011	0.095387	0.000364	0.032039	0.000100	0.000400	0.000015	0.000116	0.000023	0.000058	0.000011	0.20	0.0238	0.0047	2.4366	± 0.1000	81.9	309.2	12.7	0.00061	18.33	0.33611	0.54	0.0391	
22380B-08	7.0	290A	0.06930	0.00011	0.086935	0.000367	0.030564	0.000088	0.000408	0.000023	0.000259	0.000024	0.000071	0.000009	0.19	0.0560	0.0053	2.1490	± 0.0856	75.6	272.7	10.9	0.00082	12.14	0.35181	0.56	0.0611	
22380B-09	7.0	290A	0.06930	0.00011	0.150691	0.000448	0.036406	0.000114	0.000542	0.000020	0.000340	0.000022	0.000197	0.000010	0.23	0.0618	0.0040	2.5216	± 0.0858	61.0	320.0	10.9	0.00131	5.18	0.24174	0.48	0.1312	
22380B-10	7.0	290A	0.06930	0.00011	0.174148	0.000427	0.035825	0.000116	0.000510	0.000020	0.000174	0.000038	0.000320	0.000009	0.22	0.0322	0.0070	2.1975	± 0.0772	45.2	278.8	9.8	0.00183	2.81	0.20584	0.46	0.2342	
22380B-11	7.0	290A	0.06930	0.00011	0.190761	0.000448	0.047123	0.000134	0.000572	0.000025	0.000185	0.000030	0.000273	0.000009	0.29	0.0261	0.0043	2.3192	± 0.0611	57.3	294.3	7.8	0.00143	3.41	0.24718	0.42	0.1944	
22380B-12	7.0	290A	0.06930	0.00011	0.075860	0.000366	0.029013	0.000091	0.000411	0.000021	0.000071	0.000029	0.000028	0.000006	0.18	0.0163	0.0066	2.3304	± 0.0657	89.2	295.7	8.3	0.00036	22.56	0.38273	0.62	0.0342	
22380B-13	7.0	290A	0.06930	0.00011	0.037399	0.000309	0.014512	0.000068	0.000177	0.000015	0.000027	0.000008	0.000012	0.09	0.0076	0.0123	2.4034	± 0.2423	93.3	305.0	30.7	0.00022	140.28	0.38832	0.99	0.0070		
<i>OL04/G-4p</i>																												
24555-06	6.0	326a	0.25890	0.00082	0.073749	0.000192	0.156077	0.000271	0.001706	0.000029	0.000002	0.000022	0.000011	0.000006	1.02	-0.0003	0.0010	0.4507	± 0.0108	95.5	213.6	5.1	0.00015	49.71	2.11842	0.38	0.0139	
24555-01	6.0	326a	0.25890	0.00082	0.154139	0.000395	0.060633	0.000251	0.000813	0.000027	0.000115	0.000020	0.000366	0.000008	0.40	0.0135	0.0024	0.7404	± 0.0431	29.1	350.9	20.4	0.00237	2.34	0.39359	0.54	0.2767	
24555-02	6.0	326a	0.25890	0.00082	0.028433	0.000173	0.060286	0.000221	0.000732	0.000023	0.000015	0.000018	0.000004	0.000007	0.39	-0.0022	0.0022	0.4916	± 0.0343	104.3	233.0	16.3	- 0.00015	-166.82	2.12242	0.76	0.0051	
24555-03	6.0	326a	0.25890	0.00082	0.024883	0.000174	0.050024	0.000192	0.000544	0.000020	0.000072	0.000019	0.000004	0.000007	0.33	0.0102	0.0028	0.4744	± 0.0431	95.5	224.8	20.4	0.00015	190.37	2.01231	0.84	0.0048	
24555-04	6.0	326a	0.25890	0.00082	0.039219	0.000194	0.079543	0.000241	0.000924	0.000029	0.000040	0.000022	0.000001	0.000007	0.52	0.0032	0.0020	0.4951	± 0.0277	100.5	234.6	13.1	- 0.00002	-1090.47	2.03014	0.63	0.0007	
24555-05	6.0	326a	0.25890	0.00082	0.032093	0.000176	0.068497	0.000241	0.000820	0.000024	0.000043	0.000018	0.000006	0.000007	0.45	0.0041	0.0019	0.4925	± 0.0322	105.2	233.4	15.3	- 0.00018	-131.10	2.13650	0.70	0.0062	
24555-07	6.0	326a	0.25890	0.00082	0.073595	0.000330	0.080502	0.000371	0.000950	0.000018	0.000019	0.000024	0.000006	0.000008	0.53	-0.0022	0.0022	0.5590	± 0.0286	61.2	264.9	13.5	0.00130	7.92	1.09467	0.69	0.0916	
24555-08	6.0	326a	0.25890	0.00082	0.044211	0.000278	0.078044	0.000291	0.000874	0.000030	0.000024	0.000002	0.000007	0.01	0.0046	0.0019	0.4746	± 0.0281	83.9	224.9	13.3	0.00054	30.44	1.76687	0.78	0.0282		
24555-09	6.0	326a	0.25890	0.00082	0.029024	0.000193	0.058622	0.000241	0.000672	0.000022	0.000050	0.000021	0.000002	0.000007	0.38	-0.0068	0.0026	0.4851	± 0.0381	98.1	229.9	18.1	0.00006	399.47	2.02175	0.83	0.0022	
24555-10	6.0	326a	0.25890	0.00082	0.038964	0.000177	0.028676	0.000162	0.000364	0.000017	0.000053	0.000024	0.000007	0.000008	0.19	0.0145	0.0063	0.6182	± 0.0817	45.5	293.0	38.7	0.00182	11.00	0.73641	0.77	0.0639	
24555-12	6.0	326a	0.25890	0.00082	0.028896	0.000175	0.062970	0.000231	0.000686	0.000020	0.000010	0.000020	0.000008	0.000008	0.41	-0.0016	0.0024	0.4913	± 0.0369	107.2	232.8	17.5	- 0.00024	-111.59	2.18146	0.75	0.0076	
24555-13	6.0	326a	0.25890	0.00082	0.029514	0.000195	0.031477	0.000181	0.000361	0.000017	0.000038	0.000021	0.000042	0.000008	0.21	0.0085	0.0051	0.5425	± 0.0732	57.9	257.1	34.7	0.00141	18.46	1.06730	0.92	0.0451	
24555-14	6.0	326a	0.25890	0.00082	0.040744	0.000197	0.059409	0.000221	0.000673	0.000020	0.000001	0.000022	0.000038	0.000007	0.39	-0.0006	0.0027	0.4951	± 0.0365	72.3	234.6	17.3	0.00093	19.06	1.45935	0.66	0.0401	
24555-15	6.0	326a	0.25890	0.00082	0.045901	0.000194	0.068259	0.000221	0.000843	0.000025	0.000024	0.000019	0.000038	0.000007	0.45	-0.0030	0.0021	0.5039	± 0.0310	75.0	238.8	14.7	0.00084	18.32	1.48837	0.58	0.0405	
24555-16	6.0	326a	0.25890	0.00082	0.023136	0.000171	0.043505	0.000231	0.000494	0.000018	0.000017	0.000002	0.000003	0.000007	0.28	-0.0034	0.0035	0.4409	± 0.0458	83.0	208.9	21.7	0.00057	50.34	1.88222	0.96	0.0179	
24555-17	6.0	326a	0.25890	0.00082	0.016051	0.000161	0.035054	0.000151	0.000475	0.000020	0.000037	0.000020	0.000003	0.000007	0.23	0.0073	0.0043	0.4365	± 0.0559	95.4	206.8	26.5	0.00015	265.42	2.18608	1.14	0.0043	
24555-18	6.0	326a	0.25890	0.00082	0.025120	0.000193	0.048012	0.000241	0.000594	0.000025	0.000031	0.000018	0.000007	0.000007	0.31	-0.0052	0.0029	0.4499	± 0.0414	86.1	213.2	19.6	0.00047	56.47	1.91315	0.96	0.0165	
24555-19	6.0	326a	0.25890	0.00082	0.020065	0.000185	0.037859	0.000172	0.000390	0.000019	0.000043	0.000019	0.000003	0.000007	0.25	-0.0088	0.0037	0.5066	± 0.0529	95.7	240.1	25.1	0.00014	230.20	1.88683	1.08	0.0046	
24555-20	6.0	326a	0.25890	0.00082	0.023522	0.000156	0.051157	0.000181	0.000535	0.000019	0.000017	0.000019	0.000001	0.000007	0.33	-0.0029	0.0028	0.4535	± 0.0396	98.7	214.9	18.8	0.00004	681.04	2.17710	0.80	0.0013	
24555-21	6.0	326a	0.25890	0.00082	0.025271	0.000161	0.042766	0.000211	0.000516	0.000021	0.000024	0.000020	0.000012	0.000007	0.28	-0.0011	0.0036	0.5075	± 0.0497	86.0	240.5	23.6	0.00004	59.74	1.69388	0.85	0.0140	
24555-22	6.0	326a	0.25890	0.00082	0.028589	0.000182	0.042473</																					

TABLE DR-1 - SCTF analytical data

Lab ID#	Watts Irrad.	J (X 10 ⁻³) ± 1σ	Relative Isotopic Abundances					Derived Results					Inverse Isochron Data														
			⁴⁰ Ar ±1σ	³⁹ Ar ±1σ	³⁸ Ar ±1σ	³⁷ Ar ±1σ	³⁶ Ar ±1σ	³⁹ Ar Mol ∞ 10 ⁻¹⁵	Ca/K ±1σ	⁴⁰ Ar / ³⁹ Ar ±1σ	% ⁴⁰ Ar ±1σ	Age (Ma) ±1σ	³⁶ Ar / ⁴⁰ Ar ±%1σ	³⁹ Ar / ⁴⁰ Ar ±%1σ	³⁶ Ar / ³⁹ Ar Er. Corr.												
24556-20	6.0	326a	0.25790	0.00079	0.178128	0.000277	0.317061	0.000670	0.003754	0.000053	0.000509	0.000025	0.000085	0.000007	2.07	0.0199	0.0010	0.4822	± 0.0070	85.9	227.6	3.3	0.00047	8.52	1.78194	0.33	0.0773
24556-21	7.0	326a	0.25790	0.00079	0.062971	0.000586	0.122322	0.001001	0.001383	0.000026	0.000060	0.000015	0.000009	0.000006	3.08	0.0603	0.0155	0.4941	± 0.0165	96.2	233.3	7.8	0.00013	77.17	1.94631	1.29	0.0126
24556-22	7.0	326a	0.25790	0.00079	0.050082	0.000302	0.079929	0.000373	0.000898	0.000030	0.000133	0.000014	0.000033	0.000006	2.01	0.2041	0.0216	0.5124	± 0.0234	81.9	241.9	11.0	0.00061	20.26	1.59886	0.81	0.0405
24556-23	7.0	326a	0.25790	0.00079	0.035250	0.000245	0.057924	0.000245	0.000677	0.000022	-0.000081	0.000010	0.000014	0.000006	1.46	-0.1730	0.0215	0.5268	± 0.0319	86.7	248.7	15.1	0.00044	39.07	1.64646	0.86	0.0229
24556-24	7.0	326a	0.25790	0.00079	0.058301	0.000281	0.102435	0.000383	0.001162	0.000040	-0.000008	0.000014	0.000018	0.000006	2.58	-0.0100	0.0167	0.5162	± 0.0192	90.9	243.7	9.1	0.00031	36.37	1.76039	0.66	0.0210
24556-25	7.0	326a	0.25790	0.00079	0.038696	0.000268	0.077357	0.000323	0.000865	0.000025	-0.000054	0.000013	-0.000008	0.000006	1.95	-0.0872	0.0202	0.5271	± 0.0223	105.6	248.8	10.5	- 0.00019	-78.31	2.00311	0.85	0.0114
<i>OL04/B-W56a</i>																											
24651-01	6.0	329a	0.26200	0.00069	0.051052	0.000309	0.098917	0.000331	0.001166	0.000030	0.000040	0.000012	0.000025	0.000005	2.17	0.0022	0.0008	0.4414	± 0.0144	85.6	211.6	6.9	0.00048	18.77	1.93935	0.74	0.0453
24651-02	6.0	329a	0.26200	0.00069	0.012943	0.000210	0.028920	0.000182	0.000359	0.000015	0.000056	0.000018	-0.000002	0.000005	0.64	0.0122	0.0040	0.4662	± 0.0558	104.3	223.5	26.8	- 0.00014	-289.10	2.23659	1.80	0.0058
24651-03	6.0	329a	0.26200	0.00069	0.090995	0.000439	0.167856	0.000461	0.002063	0.000046	0.000153	0.000018	0.000044	0.000006	3.69	0.0055	0.0007	0.4641	± 0.0105	85.7	222.5	5.0	0.00048	12.84	1.84632	0.60	0.0610
24651-04	6.0	329a	0.26200	0.00069	0.058289	0.000350	0.116746	0.000371	0.001392	0.000032	0.000096	0.000017	0.000010	0.000005	2.56	0.0049	0.0010	0.4745	± 0.0143	95.1	227.5	6.8	0.00016	56.77	2.00473	0.73	0.0150
24651-05	6.0	329a	0.26200	0.00069	0.023011	0.000211	0.105898	0.000361	0.001214	0.000025	0.000748	0.000035	0.000010	0.000006	2.33	0.0457	0.0022	0.1900	± 0.0175	87.6	91.1	8.4	0.00042	64.57	4.60938	1.03	0.0169
24651-06	6.0	329a	0.26200	0.00069	0.027721	0.000216	0.058260	0.000241	0.000683	0.000021	0.000050	0.000018	-0.000001	0.000005	1.28	0.0052	0.0021	0.4798	± 0.0282	100.9	230.1	13.5	- 0.00003	-620.55	2.10370	0.93	0.0015
24651-07	6.0	329a	0.26200	0.00069	0.015865	0.000205	0.031210	0.000192	0.000398	0.000021	0.000115	0.000015	0.000008	0.000005	0.69	0.0237	0.0032	0.4309	± 0.0469	84.9	206.6	22.5	0.00051	60.26	1.96902	1.49	0.0226
24651-08	6.0	329a	0.26200	0.00069	0.091536	0.000416	0.164060	0.000422	0.001949	0.000033	0.000102	0.000020	0.000035	0.000006	3.61	0.0037	0.0008	0.4949	± 0.0122	88.8	237.3	5.9	0.00038	18.82	1.79387	0.57	0.0409
24651-09	6.0	329a	0.26200	0.00069	0.042680	0.000256	0.088545	0.000302	0.001109	0.000031	0.000308	0.000018	-0.000001	0.000006	1.95	0.0224	0.0014	0.4862	± 0.0189	101.0	233.1	9.1	- 0.00003	-400.44	2.07657	0.74	0.0021
24651-10	6.0	329a	0.26200	0.00069	0.007767	0.000185	0.059427	0.000192	0.000713	0.000023	0.000017	0.000021	0.000005	0.000005	1.31	0.0181	0.0019	0.0245	± 0.0243	18.8	11.8	11.7	0.000272	22.89	7.66899	2.48	0.1089
24651-11	6.0	329a	0.26200	0.00069	0.027862	0.000236	0.054226	0.000252	0.000615	0.000020	0.000017	0.000011	0.000005	0.000005	1.19	0.0119	0.0021	0.4521	± 0.0304	88.1	216.8	14.6	0.00040	48.98	1.94803	1.01	0.0205
24651-12	6.0	329a	0.26200	0.00069	0.021625	0.000211	0.041119	0.000142	0.000473	0.000020	0.000021	0.000016	-0.000007	0.000006	0.90	0.0030	0.0026	0.5786	± 0.0404	110.1	277.4	19.4	- 0.00034	-75.11	1.90319	1.08	0.0152
24651-13	6.0	329a	0.26200	0.00069	0.029098	0.000219	0.044751	0.000231	0.000471	0.000022	0.000091	0.000016	0.000029	0.000006	0.98	0.0130	0.0024	0.4574	± 0.0373	70.4	219.3	17.9	0.00099	19.19	1.53918	0.96	0.0477
24651-14	6.0	329a	0.26200	0.00069	0.021516	0.000222	0.044992	0.000193	0.000524	0.000020	0.000031	0.000017	-0.000020	0.000005	0.99	0.0042	0.0025	0.6114	± 0.0368	128.0	293.1	17.6	- 0.00094	-27.21	2.03099	1.16	0.0429
24651-15	6.0	329a	0.26200	0.00069	0.025592	0.000248	0.051226	0.000192	0.000592	0.000029	0.000057	0.000019	0.000007	0.000005	1.13	0.0070	0.0024	0.4599	± 0.0312	92.1	220.5	14.9	0.00026	78.40	2.00348	1.09	0.0144
24651-16	6.0	329a	0.26200	0.00069	0.036706	0.000275	0.077498	0.000301	0.000956	0.000028	0.000042	0.000017	-0.000009	0.000005	1.71	0.0032	0.0014	0.5070	± 0.0210	107.1	243.1	10.1	- 0.00024	-60.77	2.11336	0.89	0.0155
24651-17	6.0	329a	0.26200	0.00069	0.021732	0.000234	0.046917	0.000252	0.000564	0.000018	0.000075	0.000014	0.000006	0.000005	1.03	0.0102	0.0021	0.4239	± 0.0327	91.6	203.3	15.7	0.00028	83.02	2.16099	1.25	0.0142
24651-18	6.0	329a	0.26200	0.00069	0.025720	0.000235	0.051161	0.000242	0.000628	0.000019	0.000079	0.000017	0.000015	0.000005	1.13	0.0098	0.0023	0.4174	± 0.0276	83.1	200.1	13.3	0.00057	31.98	1.99099	1.07	0.0330
24651-19	6.0	329a	0.26200	0.00069	0.022276	0.000219	0.049046	0.000211	0.000552	0.000021	0.000062	0.000016	0.000005	0.000005	1.08	0.0081	0.0022	0.4259	± 0.0303	93.9	204.2	14.5	0.00021	107.25	2.20392	1.12	0.0105
24651-20	6.0	329a	0.26200	0.00069	0.019349	0.000213	0.038286	0.000163	0.000400	0.000019	0.000169	0.000019	-0.000009	0.000007	0.84	0.0291	0.0033	0.5751	± 0.0526	113.9	275.7	25.2	- 0.00047	-74.39	1.98048	1.23	0.0166
24651-21	6.0	329a	0.26200	0.00069	0.020521	0.000192	0.040719	0.000172	0.000467	0.000018	0.000065	0.000014	0.000006	0.000006	0.90	0.0102	0.0023	0.4986	± 0.0479	99.0	239.0	23.0	0.00003	968.61	1.98605	1.07	0.0011
24651-22	6.0	329a	0.26200	0.00069	0.021075	0.000219	0.044160	0.000222	0.000524	0.000021	-0.000016	0.000019	0.000005	0.000006	0.97	-0.0029	0.0028	0.4442	± 0.0381	93.2	213.0	18.3	0.00023	115.75	2.09742	1.20	0.0100
24651-23	6.0	329a	0.26200	0.00069	0.015235	0.000191	0.029971	0.000192	0.000313	0.000016	0.000147	0.000017	-0.000004	0.000005	0.66	0.0325	0.0038	0.4739	± 0.0465	93.3	227.2	22.3	0.00022	135.30	1.96915	1.46	0.0097
24651-24	6.0	329a	0.26200	0.00069	0.027165	0.000271	0.049237	0.000202	0.000557	0.000026	0.000015	0.000005	-0.000002	0.000006	1.09	0.0064	0.0021	0.4308	± 0.0327	78.2	206.6	15.7	0.00073	26.65	1.81411	1.13	0.0429
24651-25	6.0	329a	0.26200	0.00069	0.017118	0.000196	0.035654	0.000231	0.000463	0.000019	0.000029	0.000017	-0.000004	0.000006	0.79	0.0050	0.0032	0.5149	± 0.0516	107.3	246.9	24.7	- 0.00025	-145.14	2.08485	1.36	0.0084

TABLE DR-1 - SCTF analytical data

Lab ID#	Watts Irrad.	J	Relative Isotopic Abundances										Derived Results						Inverse Isochron Data								
			^{40}Ar	^{39}Ar	^{38}Ar	^{37}Ar	^{36}Ar	$^{39}\text{Ar Mol}$	Ca/K	$^{40}\text{Ar} / {}^{39}\text{Ar}$	% ^{40}Ar	Age (Ma)	$^{36}\text{Ar}/{}^{40}\text{Ar}$	$^{39}\text{Ar}/{}^{40}\text{Ar}$	$^{36}\text{Ar} / {}^{39}\text{Ar}$	$\pm\%1\sigma$	$\pm\%1\sigma$	$\pm\%1\sigma$	Er. Corr.								
		$(\text{X } 10^{-3}) \pm 1\sigma$	$\pm 1\sigma$	$\pm 1\sigma$	$\pm 1\sigma$	$\pm 1\sigma$	$\pm 1\sigma$	$\infty 10^{-15}$	$\pm 1\sigma$	$\pm 1\sigma$	$\pm 1\sigma$	$\pm 1\sigma$	$\pm 1\sigma$	$\pm 1\sigma$	$\pm 1\sigma$	$\pm 1\sigma$	$\pm 1\sigma$										
24665-07	8.0	329c	0.25610	0.00093	0.125690	0.000491	0.092126	0.000441	0.001072	0.000029	0.000880	0.000022	-0.000011	0.000006	2.09	0.0843	0.0022	1.4036	± 0.0208	103.0	657.9	9.8	- 0.00010	-46.45	0.73348	0.66	0.0149
24665-08	8.0	329c	0.25610	0.00093	0.081799	0.000363	0.156390	0.000461	0.001859	0.000031	0.000223	0.000018	0.000017	0.000005	3.55	0.0122	0.0010	0.4898	± 0.0106	93.7	229.6	5.0	0.00021	31.11	1.91381	0.58	0.0244
24665-09	8.0	329c	0.25610	0.00093	0.128159	0.000451	0.101640	0.000291	0.001196	0.000028	0.000286	0.000020	0.000025	0.000005	2.31	0.0245	0.0017	1.1877	± 0.0172	94.3	556.7	8.1	0.00019	22.09	0.79366	0.51	0.0323
24665-10	8.0	329c	0.25610	0.00093	0.051842	0.000379	0.099857	0.000352	0.001169	0.000023	0.000407	0.000018	0.000001	0.000005	2.27	0.0359	0.0016	0.5182	± 0.0162	99.9	242.9	7.6	0.00000	3385.47	1.92812	0.86	0.0003
24665-11	8.0	329c	0.25610	0.00093	0.132136	0.000512	0.090026	0.000322	0.001051	0.000032	0.000432	0.000019	0.000044	0.000005	2.05	0.0424	0.0019	1.3243	± 0.0189	90.3	620.7	8.8	0.00033	11.88	0.68179	0.58	0.0603
24665-12	8.0	329c	0.25610	0.00093	0.131241	0.000463	0.082653	0.000292	0.001051	0.000023	0.000651	0.000022	0.000066	0.000005	1.88	0.0699	0.0025	1.3520	± 0.0202	85.2	633.7	9.5	0.00050	7.79	0.63021	0.55	0.0900
24665-13	8.0	329c	0.25610	0.00093	0.048824	0.000346	0.101443	0.000391	0.001198	0.000026	0.000171	0.000015	-0.000003	0.000005	2.31	0.0148	0.0014	0.4893	± 0.0162	101.8	229.4	7.6	- 0.00006	-183.20	0.207996	0.85	0.0050
24665-14	8.0	329c	0.25610	0.00093	0.249116	0.000925	0.192068	0.000621	0.002371	0.000040	0.000990	0.000026	0.000068	0.000006	4.37	0.0461	0.0013	1.1928	± 0.0111	92.0	559.1	5.2	0.00027	8.34	0.77155	0.54	0.0858
24665-15	8.0	329c	0.25610	0.00093	0.098219	0.000430	0.078768	0.000312	0.000976	0.000034	0.000297	0.000018	0.000033	0.000005	1.79	0.0337	0.0021	1.1220	± 0.0196	90.0	525.9	9.2	0.00033	14.45	0.80255	0.64	0.0508
24664-04	7.0	329c	0.25800	0.00089	0.203957	0.000689	0.139195	0.000432	0.001657	0.000035	0.000345	0.000020	0.000047	0.000009	3.28	0.0313	0.0019	1.3645	± 0.0217	93.2	644.3	10.2	0.00023	20.43	0.68304	0.51	0.0344
24664-05	7.0	329c	0.25800	0.00089	0.263188	0.002403	0.182431	0.001801	0.002109	0.000044	0.000311	0.000021	0.000116	0.000007	4.31	0.0234	0.0015	1.2533	± 0.0221	86.9	591.8	10.4	0.00044	6.12	0.69375	1.39	0.1476
24664-06	7.0	329c	0.25800	0.00089	0.339878	0.00085	0.167948	0.000571	0.002059	0.000039	0.000749	0.000026	0.000350	0.000007	3.97	0.0584	0.0021	1.4029	± 0.0167	69.4	662.4	7.9	0.00103	2.26	0.49453	0.48	0.2924
24664-07	7.0	329c	0.25800	0.00089	0.201570	0.000439	0.165393	0.000572	0.001857	0.000037	0.000774	0.000021	0.000011	0.000007	3.91	0.0613	0.0017	1.2002	± 0.0132	98.6	566.7	6.2	0.00005	68.65	0.82124	0.46	0.0095
24664-08	7.0	329c	0.25800	0.00089	0.116728	0.000361	0.231344	0.000751	0.002721	0.000054	0.000627	0.000025	0.000014	0.000007	5.51	0.0351	0.0014	0.4833	± 0.0092	96.6	228.2	4.3	0.00011	52.50	1.9966	0.50	0.0131
24664-09	7.0	329c	0.25800	0.00089	0.150381	0.000536	0.225669	0.000781	0.002621	0.000044	0.000155	0.000020	0.000141	0.000007	5.34	0.0086	0.0012	0.4802	± 0.0104	72.1	226.8	4.9	0.00093	5.30	1.50223	0.55	0.1327
24664-10	7.0	329c	0.25800	0.00089	0.099640	0.000390	0.078206	0.000363	0.000969	0.000036	0.000224	0.000020	0.000039	0.000007	1.85	0.0374	0.0034	1.1253	± 0.0290	88.4	531.4	13.7	0.00039	18.84	0.78557	0.65	0.0369
24664-11	7.0	329c	0.25800	0.00089	0.102230	0.000352	0.077168	0.000363	0.000893	0.000025	0.000238	0.000016	0.000029	0.000008	1.82	0.0403	0.0028	1.2137	± 0.0302	91.7	573.1	14.2	0.00028	26.44	0.75549	0.63	0.0254
24664-12	7.0	329c	0.25800	0.00089	0.245578	0.000727	0.177649	0.000502	0.002087	0.000037	0.000570	0.000023	0.000121	0.000008	4.20	0.0421	0.0017	1.1795	± 0.0144	85.4	556.9	6.8	0.00049	6.36	0.72401	0.46	0.1085
24664-13	7.0	329c	0.25800	0.00089	0.097223	0.000443	0.171276	0.000522	0.002102	0.000040	0.000406	0.000022	0.000044	0.000007	4.05	0.0310	0.0017	0.4915	± 0.0134	86.7	232.1	6.3	0.00045	17.20	1.76364	0.60	0.0443
24664-14	7.0	329c	0.25800	0.00089	0.369124	0.001004	0.230165	0.000721	0.002782	0.000053	0.001012	0.000025	0.000351	0.000009	5.45	0.0580	0.0015	1.1498	± 0.0139	71.8	542.9	6.6	0.00095	2.62	0.62406	0.47	0.2573
24664-15	7.0	329c	0.25800	0.00089	0.293403	0.000886	0.190628	0.000522	0.002288	0.000047	0.000796	0.000022	0.000101	0.000008	4.51	0.0551	0.0016	1.3816	± 0.0145	89.8	652.3	6.8	0.00034	8.03	0.65025	0.46	0.0864
24664-16	7.0	329c	0.25800	0.00089	0.238021	0.000757	0.195600	0.000621	0.002313	0.000046	0.000782	0.000027	0.000017	0.000007	4.63	0.0528	0.0019	1.1923	± 0.0127	98.1	563.0	6.0	0.00006	47.21	0.82249	0.50	0.0147
24664-17	7.0	329c	0.25800	0.00089	0.252969	0.000765	0.212391	0.000611	0.002548	0.000029	0.000634	0.000021	0.000023	0.000006	5.03	0.0394	0.0013	1.1593	± 0.0107	97.4	547.4	5.0	0.00009	29.61	0.84034	0.47	0.0234
24664-18	7.0	329c	0.25800	0.00089	0.091995	0.000370	0.172426	0.000611	0.002086	0.000042	0.000171	0.000018	0.000039	0.000006	4.08	0.0128	0.0014	0.4667	± 0.0107	87.6	220.4	5.1	0.00042	15.51	1.87645	0.58	0.0467
24664-19	7.0	329c	0.25800	0.00089	0.096874	0.000321	0.197747	0.000681	0.002302	0.000047	0.000188	0.000015	0.000014	0.000006	4.68	0.0123	0.0010	0.4691	± 0.0095	95.9	221.5	4.5	0.00014	45.50	2.04371	0.53	0.0153
24664-20	7.0	329c	0.25800	0.00089	0.128087	0.000419	0.259343	0.001001	0.002953	0.000050	0.001041	0.000022	0.000023	0.000007	6.14	0.0533	0.0012	0.4691	± 0.0082	95.1	221.5	3.9	0.00016	32.10	2.02712	0.56	0.0213
<i>OL05/Olt-Sp</i>																											
24980-01	6.0	359B	0.13120	0.00031	0.015582	0.000266	0.016073	0.000077	0.000218	0.000018	-0.000001	0.000096	0.000012	0.000010	0.19	-0.0010	0.0956	0.7459	± 0.1816	77.0	179.1	43.6	0.00077	81.23	1.03252	1.83	0.0221
24980-02	6.0	359B	0.13120	0.00031	0.028592	0.000287	0.020722	0.000076	0.000241	0.000018	-0.000002	0.000096	0.000029	0.000010	0.24	-0.0019	0.0743	0.9660	± 0.1449	70.1	232.0	34.8	0.00100	34.95	0.72542	1.12	0.0331
24980-03	6.0	359B	0.13120	0.00031	0.019035	0.000297	0.020156	0.000154	0.000210	0.000023	0.001900	0.000098	0.000007	0.000010	0.24	0.1498	0.0782	0.8436	± 0.1443	89.4	202.6	34.6	0.00035	143.54	1.05988	1.80	0.0110
24980-04	6.0																										

TABLE DR1-2 - SCTF Isochron Results

Run ID	Sample	Irradiation	<i>J</i>	$\pm J$	Weighted-Mean Ca/K	\pm Ca/K (1 σ)	Isochron Results							
							Age	\pm Age (2 σ)	<i>n</i> Included	<i>n</i> total	(^{40}Ar / ^{36}Ar) _{tr}	\pm (^{40}Ar / ^{36}Ar) _{tr}	MSWD	Probability
22377	01-STOLT11A/ALD	290A	0.00007023	0.00000011	0.0755	0.0006	168.4	2.8	13	14	292.3	6.1	0.70	0.74
22378	01-STC8A/ALD	290A	0.00006980	0.00000011	0.0979	0.0008	92.9	2.2	16	19	295.6	9.1	0.58	0.88
22380, 22380B	OLT01/ALD1-p2	290A	0.00006934	0.00000011	0.0838	0.0015	290.5	6.2	22	30	317.8	6	0.92	0.57
24555, 24556	OL04/G-4p	326a	0.00025895	0.00000082	0.0979	0.0033	225.7	4.0	52	57	350	21.6	0.91	0.65
24651	OL04/B-WS6a	329a	0.00026199	0.00000069	0.0588	0.0029	224.9	6.4	33	41	312.3	23.1	1.36	0.09
24664, 24665	OL04/g-8	329c	0.00025805	0.00000089	0.0468	0.0009	224.6	4.8	9	35	311.9	21.1	0.83	0.57
24980	OL05/Olt-8p	359B	0.00013123	0.00000031	0.2421	0.0668	190	22	18	29	296.6	27.5	0.53	0.94

TABLE DR1-3 - SCIH analytical data

Lab ID#	Watts	Irrad.	<i>J</i> (X 10 ⁻³) ± 1σ	Relative Isotopic Abundances								Derived Results								Inverse Isochron Data			
				⁴⁰ Ar ±1σ	³⁹ Ar ±1σ	³⁸ Ar ±1σ	³⁷ Ar ±1σ	³⁶ Ar ±1σ	³⁹ Ar Mol ∞ 10 ⁻¹⁵ of total	³⁹ Ar % of total	Ca/K ±1σ	⁴⁰ Ar/ ³⁹ Ar ±1σ	% ⁴⁰ Ar*	Age (Ma) ±1σ	³⁶ Ar/ ⁴⁰ Ar ±%1σ	³⁹ Ar/ ⁴⁰ Ar ±%1σ	³⁶ Ar/ ³⁹ Ar Er. Corr.						
<i>OL04/G-4p</i>																							
26074-01A	0.8	416A	0.14320 0.00028	7701.0	639.4	364.9	4.6	29.0	13.6	55.0	13.9	20.4	2.5	0.005	0.3	1.362	0.344	4.49981	2.70376	21.3	1178.9	708.1	0.002635 14.9
26074-01B	1	416A	0.14320 0.00028	6243.1	554.4	1961.2	7.9	83.7	7.7	-6.3	10.1	16.4	2.3	0.027	1.7	-0.031	0.048	0.68757	0.45308	21.6	180.2	118.7	0.002626 16.8
26074-01C	1.3	416A	0.14320 0.00028	7792.1	554.9	6724.2	13.3	146.5	12.4	12.5	10.1	7.2	2.3	0.092	5.8	0.017	0.014	0.84140	0.13290	72.7	220.5	34.8	0.000916 33.7
26074-01D	1.6	416A	0.14320 0.00028	14202.6	556.5	15788.5	21.9	229.5	13.9	-39.4	10.1	1.8	2.3	0.217	13.6	-0.024	0.006	0.86339	0.05589	96.1	226.3	14.6	0.000132 122.7
26074-01E	2.6	416A	0.14320 0.00028	27436.4	554.0	32045.3	36.6	404.4	34.5	-30.0	16.2	0.1	2.3	0.440	27.6	-0.009	0.005	0.85433	0.02769	99.9	223.9	7.3	0.000004 1972.7
26074-01F	6	416A	0.14320 0.00028	50223.5	552.9	59333.9	55.8	937.5	10.8	55.2	17.4	-1.5	2.1	0.815	51.1	0.008	0.003	0.85379	0.01419	101.0	223.7	3.7	-0.000032 -132.3
<i>OL04/G-4p - Aliquot #2</i>																							
26074-02A	0.8	416A	0.14320 0.00028	6041.2	639.4	131.3	4.0	20.5	13.6	28.6	13.9	20.3	2.3	0.002	0.1	1.968	0.958	-0.10332	7.17109	-0.2	-27.1	1879.4	0.003357 15.6
26074-02B	1	416A	0.14320 0.00028	2537.2	554.2	845.7	5.7	27.2	14.0	-12.6	16.9	6.2	2.4	0.012	0.9	-0.140	0.187	0.82009	1.05688	27.4	214.9	276.9	0.002433 43.9
26074-02C	1.3	416A	0.14320 0.00028	4398.4	558.7	4065.4	12.8	80.7	10.3	86.1	17.8	4.9	2.1	0.056	4.3	0.198	0.041	0.73267	0.20896	67.8	192.0	54.8	0.001080 46.9
26074-02D	1.6	416A	0.14320 0.00028	13940.5	563.9	14223.6	22.3	220.4	17.4	55.6	17.7	2.1	2.4	0.195	15.0	0.036	0.012	0.93726	0.06331	95.7	245.6	16.6	0.000144 117.5
26074-02E	2.6	416A	0.14320 0.00028	40923.0	569.2	42096.6	40.3	690.3	24.9	53.2	17.7	-2.9	2.3	0.578	44.3	0.011	0.004	0.99277	0.02119	102.2	260.2	5.6	-0.000074 -75.9
26074-02F	6	416A	0.14320 0.00028	38668.7	569.3	33606.2	37.3	503.1	21.1	10.4	17.2	23.5	2.3	0.462	35.4	0.002	0.005	0.94096	0.02646	81.8	246.6	6.9	0.000608 9.8
<i>OL04/G-4p - Aliquot #3</i>																							
26074-03A	0.8	416A	0.14320 0.00028	5785.7	639.8	404.6	5.1	40.9	14.1	13.3	13.8	13.5	2.2	0.006	0.4	0.296	0.308	4.34587	2.27952	30.4	1138.6	597.0	0.002331 19.9
26074-03B	1	416A	0.14320 0.00028	14036.6	568.8	2396.7	8.9	65.6	13.1	-81.3	16.2	26.9	2.3	0.033	2.6	-0.319	0.064	2.49599	0.37146	42.6	654.0	97.3	0.001921 9.4
26074-03C	1.3	416A	0.14320 0.00028	30251.4	569.5	16002.5	24.8	266.1	15.0	91.4	19.2	47.9	2.4	0.220	17.6	0.053	0.011	0.99891	0.05730	52.9	261.8	15.0	0.001578 5.4
26074-03D	1.6	416A	0.14320 0.00028	37683.8	573.2	31984.5	40.0	438.2	23.0	-1.4	27.8	5.9	4.2	0.251	35.1	-0.001	0.008	1.12193	0.04297	95.3	294.0	11.3	0.000157 70.6
26074-03E	2.6	416A	0.14320 0.00028	30315.3	572.5	24880.8	38.4	311.9	20.9	58.4	28.9	-4.3	3.8	0.195	27.3	0.022	0.011	1.27014	0.05111	104.3	332.8	13.4	-0.000145 -86.6
26074-03F	6	416A	0.14320 0.00028	21864.8	571.8	15404.6	32.6	238.4	15.9	82.5	29.1	-3.5	4.0	0.121	16.9	0.050	0.018	1.48747	0.08608	104.9	389.8	22.6	-0.000163 -112.3
<i>OL04/G-4p - Aliquot #4</i>																							
26074-04A	0.8	416A	0.14320 0.00028	3160.5	638.7	144.0	4.4	39.0	10.6	-17.7	13.7	15.6	2.5	0.002	0.1	-1.113	0.861	-10.49914	6.82713	-47.9	-2753.6	1791.9	0.004954 25.8
26074-04B	1.3	416A	0.14320 0.00028	8573.7	533.9	9035.7	14.7	93.8	12.6	51.6	28.5	0.9	2.2	0.124	5.9	0.054	0.030	0.92145	0.09243	97.2	241.5	24.2	0.000094 267.1
26074-04C	1.6	416A	0.14320 0.00028	35908.4	536.1	42027.3	44.2	645.2	11.9	-10.1	25.6	1.9	2.2	0.577	27.6	-0.003	0.006	0.84002	0.02027	98.4	220.1	5.3	0.000054 115.5
26074-04D	2.6	416A	0.14320 0.00028	76453.2	536.2	92100.5	79.6	1395.3	24.3	158.5	29.4	1.8	2.1	1.265	60.5	0.016	0.003	0.82431	0.00903	99.4	216.0	2.4	0.000020 135.7
26074-04E	6	416A	0.14320 0.00028	7774.7	533.5	8927.1	17.6	175.5	6.0	-51.8	24.2	1.1	2.2	0.123	5.9	-0.057	0.026	0.82979	0.09357	95.4	217.5	24.5	0.000155 178.7
<i>OL04/G-4p - Aliquot #5</i>																							
26074-05A	0.8	416A	0.14320 0.00028	2275.8	637.8	65.9	3.9	-15.6	14.4	-18.3	13.8	7.8	2.4	0.001	0.1	-2.518	1.898	-0.75393	14.51023	-2.2	-197.6	3803.1	0.003423 41.6
26074-05B	1	416A	0.14320 0.00028	10134.5	533.1	2483.3	8.6	55.6	11.4	86.6	29.2	3.6	2.1	0.034	4.5	0.333	0.112	3.66262	0.33307	89.8	959.6	87.2	0.000342 61.3
26074-05C	1.3	416A	0.14320 0.00028	7664.9	531.8	5951.0	12.4	77.3	9.4	-70.3	23.6	5.7	2.2	0.082	10.7	-0.115	0.038	0.99887	0.14044	77.6	261.8	36.8	0.000750 38.3
26074-05D	1.6	416A	0.14320 0.00028	16611.6	531.3	17743.9	21.6	268.6	14.9	3.5	25.3	5.9	2.1	0.244	32.0	0.001	0.014	0.83634	0.04665	89.4	219.2	12.2	0.000355 36.3
26074-05E	2.4	416A	0.14320 0.00028	20810.8	530.5	23672.8	27.4	320.6	12.0	57.2	26.7	-0.3	2.1	0.325	42.6	0.023	0.011	0.88312	0.03494	100.5	231.4	9.2	-0.000018 -560.7
26074-05F	6	416A	0.14320 0.00028	5331.5	527.6	5597.3	13.3	150.8	15.3	88.9	27.5	3.3	2.2	0.077	10.1	0.154	0.048	0.78013	0.15174	82.0	204.4	39.8	0.000604 70.0

TABLE DR1-3 - SCIH analytical data

Lab ID#	Watts	Irrad.	<i>J</i> (X 10 ⁻³) ± 1σ	Relative Isotopic Abundances								Derived Results								Inverse Isochron Data							
				⁴⁰ Ar ±1σ	³⁹ Ar ±1σ	³⁸ Ar ±1σ	³⁷ Ar ±1σ	³⁶ Ar ±1σ	³⁹ Ar Mol ∞ 10 ⁻¹⁵	³⁹ Ar % of total	Ca/K ±1σ	⁴⁰ Ar/ ³⁹ Ar ±1σ	% ⁴⁰ Ar*	Age (Ma) ±1σ	³⁶ Ar/ ⁴⁰ Ar ±%1σ	³⁹ Ar/ ⁴⁰ Ar ±%1σ	³⁶ Ar/ ³⁹ Ar Er. Corr.										
<i>OL04/G-4p - Aliquot #6</i>																											
26074-06A	0.8	416A	0.14320 0.00028	2604.9	636.5	218.3	4.6	-1.5	10.7	50.8	14.2	6.3	2.3	0.003	0.3	2.105	0.591	3.37996	4.31588	28.3	885.6	1130.5	0.002401	44.5	0.08379	24.5	0.547
26074-06B	1	416A	0.14320 0.00028	2062.4	531.7	1109.3	6.7	9.7	8.2	55.4	27.7	1.2	2.3	0.015	1.5	0.477	0.239	1.56632	0.77851	84.3	410.4	204.0	0.000526	211.8	0.53815	25.8	0.122
26074-06C	1.3	416A	0.14320 0.00028	6779.8	526.4	7020.4	14.6	156.2	17.3	169.8	29.8	0.3	2.1	0.096	9.7	0.234	0.041	0.96111	0.11740	99.6	251.9	30.8	0.000014	2322.6	1.03626	7.8	0.003
26074-06D	1.6	416A	0.14320 0.00028	14521.9	525.3	16053.3	23.2	234.0	31.5	271.3	32.5	0.4	2.1	0.220	22.2	0.164	0.020	0.90373	0.05099	100.0	236.8	13.4	0.000001	27680.3	1.10633	3.6	0.000
26074-06E	2.4	416A	0.14320 0.00028	17805.4	523.5	20334.6	25.0	293.9	12.6	101.1	29.6	0.6	2.2	0.279	28.1	0.048	0.014	0.86818	0.04139	99.2	227.5	10.8	0.000026	484.7	1.14301	2.9	0.006
26074-06F	6	416A	0.14320 0.00028	24412.2	523.5	27569.5	30.8	444.0	17.3	433.5	36.7	-2.6	2.2	0.379	38.1	0.152	0.013	0.91890	0.03073	103.9	240.8	8.1	-0.000129	-70.8	1.13024	2.1	0.030
<i>OL04/G-4p - Aliquot #7</i>																											
26074-07A	0.8	416A	0.14320 0.00028	1603.9	634.3	68.7	3.9	-11.0	7.5	-23.0	13.8	3.3	2.4	0.001	0.1	-3.032	1.828	8.71158	14.04098	37.3	2281.6	3675.2	0.002098	82.5	0.04287	39.9	0.475
26074-07B	1	416A	0.14320 0.00028	2368.2	536.1	1720.4	7.0	20.9	8.7	-13.2	26.3	3.0	2.3	0.024	2.6	-0.074	0.146	0.85373	0.50342	62.1	223.7	131.9	0.001270	79.1	0.72703	22.6	0.286
26074-07C	1.3	416A	0.14320 0.00028	11493.0	542.0	11267.4	20.0	170.5	13.4	-114.8	24.0	4.0	2.3	0.155	17.3	-0.099	0.021	0.90819	0.07767	89.1	238.0	20.4	0.000365	55.2	0.98121	4.7	0.085
26074-07D	1.6	416A	0.14320 0.00028	17207.2	527.4	19617.6	25.8	271.2	14.6	46.9	27.9	-0.9	2.3	0.269	30.1	0.023	0.014	0.89155	0.04423	101.7	233.6	11.6	-0.000058	-231.3	1.14105	3.1	0.013
26074-07E	2.4	416A	0.14320 0.00028	19376.8	532.9	22033.1	37.1	817.8	45.4	-7.1	26.4	-1.4	2.2	0.303	33.8	-0.004	0.012	0.89806	0.03789	102.2	235.3	9.9	-0.000074	-150.3	1.13806	2.8	0.018
26074-07F	6	416A	0.14320 0.00028	8787.2	537.6	10566.1	17.4	190.6	15.8	43.7	27.6	1.2	2.2	0.145	16.2	0.040	0.025	0.79858	0.07935	96.1	209.3	20.8	0.000130	188.5	1.20348	6.1	0.032
<i>OL04/G-4p - Aliquot #8</i>																											
26074-08A	0.8	416A	0.14320 0.00028	4872.5	632.6	131.4	3.8	-8.7	7.7	-78.9	13.3	15.5	2.3	0.002	0.1	-5.426	0.927	1.66391	7.06268	4.5	436.0	1850.5	0.003199	19.6	0.02703	13.3	0.648
26074-08B	1	416A	0.14320 0.00028	2207.6	541.4	793.0	5.7	-8.9	11.4	1.6	27.0	-3.5	2.2	0.011	0.7	0.019	0.325	4.08461	1.08063	146.8	1070.1	283.0	-0.001568	-68.8	0.35945	24.5	0.356
26074-08C	1.3	416A	0.14320 0.00028	5791.2	548.2	5081.4	13.1	53.0	17.4	41.4	27.3	1.1	1.8	0.070	4.3	0.079	0.052	1.07871	0.15064	94.7	282.7	39.5	0.000177	175.3	0.87811	9.5	0.054
26074-08D	1.6	416A	0.14320 0.00028	19604.5	554.9	22606.3	26.2	324.0	20.9	31.2	27.8	-0.7	2.3	0.310	19.1	0.013	0.012	0.87587	0.03954	101.1	229.5	10.4	-0.000036	-329.0	1.15411	2.8	0.009
26074-08E	2.4	416A	0.14320 0.00028	52564.9	561.8	63278.4	47.6	881.5	24.5	-37.1	25.6	-3.1	2.2	0.869	53.5	-0.006	0.004	0.84423	0.01356	101.7	221.2	3.6	-0.000058	-71.7	1.20487	1.1	0.015
26074-08F	6	416A	0.14320 0.00028	22006.9	554.8	26493.2	29.2	365.2	14.3	-158.3	23.0	1.7	2.2	0.364	22.4	-0.059	0.008	0.80877	0.03249	97.5	211.9	8.5	0.000085	117.6	1.20494	2.5	0.021
<i>OL04/G-4p - Aliquot #9</i>																											
26074-09A	0.8	416A	0.14320 0.00028	7227.5	631.2	114.1	4.3	-6.2	6.9	-38.5	13.5	23.9	2.3	0.002	0.1	-3.057	1.077	0.62019	8.15525	1.0	162.5	2137.1	0.003317	13.0	0.01581	9.5	0.619
26074-09B	1	416A	0.14320 0.00028	2665.8	547.0	937.7	6.1	24.7	15.4	-0.8	26.7	6.4	2.1	0.013	0.7	-0.008	0.273	0.79964	0.89361	28.1	209.5	234.2	0.002407	39.0	0.35197	20.5	0.526
26074-09C	1.3	416A	0.14320 0.00028	5037.6	547.0	4706.5	11.5	71.3	11.3	-31.3	25.9	2.2	2.6	0.065	3.6	-0.065	0.054	0.92714	0.19941	86.7	243.0	52.3	0.000446	114.4	0.93505	10.9	0.095
26074-09D	1.6	416A	0.14320 0.00028	21550.3	540.7	21077.3	26.1	316.6	28.9	43.1	28.3	9.2	2.3	0.289	16.3	0.019	0.013	0.89230	0.04112	87.3	233.8	10.8	0.000424	25.0	0.97885	2.5	0.100
26074-09E	2.4	416A	0.14320 0.00028	45717.1	531.8	38698.9	37.6	556.7	23.6	45.0	27.8	38.4	2.5	0.532	29.9	0.011	0.007	0.88496	0.02361	75.0	231.9	6.2	0.000838	6.6	0.84715	1.2	0.176
26074-09F	6	416A	0.14320 0.00028	68281.5	529.8	64036.9	53.6	946.2	26.1	96.4	29.1	46.1	2.5	0.880	49.4	0.014	0.004	0.85146	0.01416	79.9	223.1	3.7	0.000673	5.4	0.93859	0.8	0.143
<i>OL04/G-4p - Aliquot #10</i>																											
26074-10A	0.8	416A	0.14320 0.00028	4907.1	630.0	100.8	4.0	15.4	8.3	-38.3	13.5	13.9	2.5	0.001	0.1	-3.435	1.217	7.46247	9.66263	15.4	1954.7	2529.6	0.002835	22.0	0.02058	13.4	0.557
26074-10B	1	416A	0.14320 0.00028	1859.8	555.5	733.6	6.0	54.9	15.9	-150.7	23.3	3.4	2.3	0.010	0.8	-1.964	0.304	1.09374	1.21291	43.2	286.6	317.8	0.001903	72.4	0.39496	29.9	0.413
26074-10C	1.3	416A	0.14320 0.00028	4451.6	525.5	4404.8	12.3	44.3	16.2	63.5	28.0	4.1	2.5	0.060	4.6	0.140	0.062	0.73536	0.20708	72.8	192.7	54.3	0.000910	62.8	0.99026	11.8	0.188
26074-10D	1.6	416A	0.14320 0.00028	23593.9	523.9	27262.2	31.3	396.2	16.0	171.2	30.7	-0.6	2.4	0.374	28.7	0.061	0.011	0.87406	0.03293	101.1	229.1	8.6	-0.000036	-285.5	1.15645	2.2	0.008
26074-10E	2.4	416A	0.14320 0.00028	32878.1	524.8	38896.3	42.0	502.0	16.0	235.2	32.4	-0.1	2.2	0.534	40.9	0.058	0.008	0.84749	0.02178	100.3	222.1	5.7	-0.000012	-579.6	1.18405	1.6	0.003
26074-10F	6	416A	0.14320 0.00028	20134.8	522.1	23657.2	30.0	415.1	25.6	34.0	10.9	0.4	2.2	0.325	24.9	0.014	0.004	0.84558	0.03586	99.4	221.6	9.4	0.000019	591.8	1.17596	2.6	0.004

TABLE DR1-3 - SCIH analytical data

Lab ID#	Watts	Irrad.	J	Relative Isotopic Abundances								Derived Results								Inverse Isochron Data								
				^{40}Ar	$\pm 1\sigma$	^{39}Ar	$\pm 1\sigma$	^{38}Ar	$\pm 1\sigma$	^{37}Ar	$\pm 1\sigma$	^{36}Ar	$\pm 1\sigma$	^{39}Ar Mol $\infty 10^{-15}$	^{39}Ar % of total	Ca/K	$^{40}\text{Ar}/^{39}\text{Ar}$	$\pm 1\sigma$	$\%^{40}\text{Ar}^*$	Age (Ma)	$\pm 1\sigma$	$^{36}\text{Ar}/^{40}\text{Ar}$	$\pm 1\sigma$	$^{39}\text{Ar}/^{40}\text{Ar}$	$\pm 1\sigma$	$^{36}\text{Ar}/^{39}\text{Ar}$	Er. Corr.	
<i>OL04/G-4p - Aliquot #11</i>																												
26074-11A	0.8	416A	0.14320	0.00028	161.7	199.6	10.7	2.5	0.0	0.0	12.7	10.2	3.9	1.6	0.000	0.0	31.032	26.036	-92.83946	53.34286	-609.0	-24493.8	14168.0	0.023749	130.2	0.06560	125.6	0.931
26074-11B	1	416A	0.14320	0.00028	416.2	199.7	165.2	2.6	0.0	0.0	1.8	10.4	3.0	1.5	0.002	0.2	0.275	1.629	-2.89597	2.97210	-115.1	-759.1	779.2	0.007203	69.4	0.39733	48.0	0.691
26074-11C	1.3	416A	0.14320	0.00028	4171.0	201.3	2572.8	10.3	0.0	0.0	-7.9	10.3	8.3	1.4	0.035	2.5	-0.081	0.104	0.65569	0.18284	40.5	171.8	47.9	0.001993	17.8	0.61751	4.8	0.270
26074-11D	1.6	416A	0.14320	0.00028	13770.4	202.4	13845.1	26.5	0.0	0.0	2.7	10.3	9.9	1.5	0.190	13.6	0.005	0.019	0.78017	0.03494	78.5	204.4	9.2	0.000719	14.9	1.00661	1.5	0.098
26074-11E	2.6	416A	0.14320	0.00028	25277.6	204.0	27051.1	37.1	0.0	0.0	-0.7	10.3	9.7	1.8	0.371	26.6	-0.001	0.010	0.82595	0.02082	88.5	216.4	5.5	0.000385	18.1	1.07144	0.8	0.044
26074-11F	6	416A	0.14320	0.00028	40638.2	205.3	44146.8	45.6	0.0	0.0	22.1	10.3	10.8	1.5	0.605	43.5	0.013	0.006	0.84712	0.01109	92.1	222.0	2.9	0.000263	13.9	1.08764	0.5	0.036
26074-11G	8	416A	0.14320	0.00028	14905.6	201.6	13802.9	25.4	0.0	0.0	7.5	10.4	11.6	1.3	0.189	13.6	0.014	0.020	0.82917	0.03260	76.9	217.3	8.5	0.000775	11.7	0.92709	1.4	0.114
<i>OL04/G-4p - Aliquot #12</i>																												
26074-12A	0.8	416A	0.14320	0.00028	-24.3	198.7	-5.7	2.0	0.0	0.0	-3.5	10.2	2.6	1.4	0.000	0.0	16.100	47.156	140.21000	95.17470	3258.1	36381.1	24451.7	-0.105777	-817.8	0.23237	816.8	0.997
26074-12B	1	416A	0.14320	0.00028	310.6	197.2	63.8	2.6	0.0	0.0	5.1	10.3	1.0	1.3	0.001	0.1	2.075	4.192	0.09510	6.86577	2.0	24.9	1799.3	0.003284	143.4	0.20553	63.6	0.442
26074-12C	1.3	416A	0.14320	0.00028	5480.7	197.0	2713.0	9.9	0.0	0.0	14.6	10.0	0.5	1.4	0.037	4.2	0.139	0.095	1.97242	0.16809	97.7	516.8	44.0	0.000076	331.5	0.49551	3.6	0.011
26074-12D	1.6	416A	0.14320	0.00028	14363.7	189.8	12498.6	21.5	0.0	0.0	-2.5	10.0	7.4	1.2	0.171	19.2	-0.006	0.021	0.97074	0.03259	84.6	254.4	8.5	0.000517	16.3	0.87115	1.3	0.080
26074-12E	2.6	416A	0.14320	0.00028	24896.8	192.9	25708.3	32.0	0.0	0.0	22.4	9.9	6.6	1.3	0.352	39.6	0.022	0.010	0.89205	0.01681	92.2	233.8	4.4	0.000261	20.0	1.03381	0.8	0.038
26074-12F	6	416A	0.14320	0.00028	25146.8	190.2	19375.1	31.5	0.0	0.0	-0.3	9.8	22.3	1.3	0.265	29.8	-0.001	0.013	0.95253	0.02201	73.5	249.6	5.8	0.000889	5.8	0.77134	0.8	0.128
26074-12G	8	416A	0.14320	0.00028	5269.8	186.6	4586.1	13.0	0.0	0.0	11.1	9.9	4.3	1.2	0.063	7.1	0.063	0.056	0.87263	0.08593	76.0	228.7	22.5	0.000803	27.7	0.87124	3.6	0.127
<i>OL04/G-4p - Aliquot #13</i>																												
26074-13A	0.8	416A	0.14320	0.00028	5324.8	186.0	241.7	4.1	0.0	0.0	6.8	10.0	20.8	1.3	0.003	0.3	0.733	1.075	-3.63528	1.77068	-16.5	-953.0	464.3	0.003903	7.1	0.04543	3.9	0.441
26074-13B	1	416A	0.14320	0.00028	4207.3	184.4	1097.6	6.9	0.0	0.0	0.7	9.9	9.4	1.6	0.015	1.2	0.016	0.236	1.27606	0.46322	33.3	334.4	121.4	0.002233	17.5	0.26113	4.4	0.248
26074-13C	1.3	416A	0.14320	0.00028	5950.7	184.3	3646.1	12.3	0.0	0.0	0.1	10.2	8.9	1.3	0.050	4.0	0.000	0.073	0.90587	0.11920	55.6	237.4	31.2	0.001488	15.2	0.61338	3.1	0.202
26074-13D	1.6	416A	0.14320	0.00028	10652.6	183.6	8091.8	19.8	0.0	0.0	-4.0	10.1	13.4	1.2	0.111	8.9	-0.013	0.033	0.82186	0.05019	62.5	215.4	13.2	0.001256	9.2	0.76045	1.7	0.185
26074-13E	2.6	416A	0.14320	0.00028	69405.9	192.6	65766.2	63.5	0.0	0.0	-12.0	10.2	48.3	1.7	0.901	72.2	-0.005	0.004	0.83488	0.00842	79.2	218.8	2.2	0.000697	3.6	0.94866	0.3	0.073
26074-13F	6	416A	0.14320	0.00028	24065.5	188.6	9242.9	18.7	0.0	0.0	-23.5	10.3	56.2	1.6	0.127	10.1	-0.067	0.029	0.78418	0.05687	30.1	205.5	14.9	0.002340	3.0	0.38448	0.8	0.251
26074-13G	8	416A	0.14320	0.00028	5045.8	184.8	3026.7	10.3	0.0	0.0	-13.9	10.4	7.1	1.5	0.041	3.3	-0.120	0.090	0.96266	0.16125	57.8	252.3	42.3	0.001413	21.6	0.60051	3.7	0.169
<i>OL04/G-4p - Aliquot #14</i>																												
26074-14A	0.8	416A	0.14320	0.00028	56.7	184.1	1.7	1.9	0.0	0.0	-32.0	10.6	-0.5	1.5	0.000	0.0	-411.045	403.335	90.12233	249.35230	323.0	23467.4	64515.6	-0.007470	-476.2	0.03584	337.5	0.656
26074-14B	1	416A	0.14320	0.00028	886.1	184.1	442.2	4.6	0.0	0.0	-15.2	10.5	0.5	1.5	0.006	0.5	-0.898	0.620	1.65653	1.06905	82.8	434.1	280.1	0.000577	286.6	0.49973	20.8	0.072
26074-14C	1.3	416A	0.14320	0.00028	5609.2	186.1	4573.6	14.3	0.0	0.0	-5.5	10.3	9.3	1.5	0.063	4.9	-0.032	0.059	0.61956	0.10660	50.6	162.4	27.9	0.001655	16.6	0.81630	3.3	0.199
26074-14D	1.6	416A	0.14320	0.00028	19806.8	185.8	22076.0	29.2	0.0	0.0	-29.5	10.4	3.9	1.5	0.302	23.5	-0.035	0.012	0.84155	0.02218	93.9	220.5	5.8	0.000204	37.6	1.11593	0.9	0.025
26074-14E	2.6	416A	0.14320	0.00028	47288.4	189.0	33615.0	46.9	0.0	0.0	-12.1	10.4	65.8	1.7	0.460	35.8	-0.010	0.008	0.82124	0.01637	58.4	215.2	4.3	0.001392	2.7	0.71164	0.4	0.143
26074-14F	6	416A	0.14320	0.00028	30694.5	191.5	31011.4	38.2	0.0	0.0	9.5	10.5	12.2	1.5	0.425	33.0	0.008	0.009	0.87162	0.01531	88.2	228.4	4.0	0.000396	12.0	1.01152	0.6	0.051
26074-14G	8	416A	0.14320	0.00028	3156.8	187.7	2304.0	14.2	0.0	0.0	-30.5	10.3	4.4	1.4	0.032	2.5	-0.347	0.117	0.78030	0.19358	57.0	204.5	50.7	0.001440	30.4	0.73073	6.0	0.194
<i>OL10/BOK2-4b</i>																												
26028-01A	1.1	413B	0.01710	0.00007	68090.7	250.6	1318.5	5.9	51.2	8.7	2.1	19.4	154.4	3.0	0.015	27.0	0.004	0.044	16.68719	0.70340	32.3	522.7	22.0	0.002267	2.0	0.01937	0.6	0.120
26028-01B	1.2	413B	0.01710	0.00007	15866.7	227.8	901.7	5.5	13.2	9.0	23.5	18.7	2.1	2.1	0.010	18.5	0.090	0.072	16.91277	0.75994	96.1	529.8	23.8	0.000129				

TABLE DR1-3 - SCIH analytical data

Lab ID#	Watts	Irrad.	J ($\times 10^{-3}$) $\pm 1\sigma$	Relative Isotopic Abundances								Derived Results								Inverse Isochron Data							
				^{40}Ar $\pm 1\sigma$	^{39}Ar $\pm 1\sigma$	^{38}Ar $\pm 1\sigma$	^{37}Ar $\pm 1\sigma$	^{36}Ar $\pm 1\sigma$	^{39}Ar Mol $\times 10^{-15}$	^{39}Ar % of total	Ca/K	$^{40}\text{Ar}/^{39}\text{Ar}$ $\pm 1\sigma$	% $^{40}\text{Ar}^*$ $\pm 1\sigma$	Age (Ma) $\pm 1\sigma$	$^{36}\text{Ar}/^{40}\text{Ar}$ $\pm 1\sigma$	$^{39}\text{Ar}/^{40}\text{Ar}$ $\pm 1\sigma$	$^{36}\text{Ar}/^{39}\text{Ar}$ Er. Corr.										
26028-01F	4.5	413B	0.01710 0.00007	20444.4	231.2	1234.1	5.5	41.0	21.3	13.7	18.6	0.4	2.1	0.014	25.3	0.039	0.054	16.46109	0.54807	99.4	515.6	17.2	0.000021	503.0	0.06038	1.2	0.002

OL10/BOK2-4b - Aliquot #2

26028-02A	1.1	413B	0.01710 0.00007	28453.3	244.6	1008.4	5.1	28.0	8.5	25.9	19.3	68.3	2.6	0.012	10.1	0.076	0.057	7.99038	0.80211	28.3	250.3	25.1	0.002401	3.9	0.03544	1.0	0.191
26028-02B	1.2	413B	0.01710 0.00007	9506.0	229.0	817.2	5.1	24.9	7.9	4.5	18.6	5.0	2.2	0.009	8.2	0.019	0.081	9.81429	0.86740	84.4	307.4	27.2	0.000523	45.2	0.08599	2.5	0.052
26028-02C	1.5	413B	0.01710 0.00007	21983.5	233.9	1889.5	7.1	17.5	10.7	-9.2	18.7	22.7	2.3	0.021	19.0	-0.018	0.035	8.05148	0.38166	69.2	252.2	12.0	0.001031	10.1	0.08597	1.1	0.099
26028-02D	2.6	413B	0.01710 0.00007	45427.7	240.9	5642.7	13.1	67.3	12.4	-12.4	18.7	3.6	2.3	0.064	56.7	-0.008	0.012	7.85638	0.13022	97.6	246.1	4.1	0.000080	63.3	0.12424	0.6	0.008
26028-02E	4.5	413B	0.01710 0.00007	5413.9	242.8	593.4	3.9	5.0	8.9	14.4	18.6	2.0	2.3	0.007	6.0	0.086	0.112	8.11013	1.20538	88.9	254.1	37.8	0.000371	112.1	0.10964	4.5	0.040

OL10/BOK2-4b - Aliquot #3

26028-03A	1.1	413B	0.01710 0.00007	35508.1	243.4	1397.1	5.5	2.6	11.8	55.1	19.3	86.9	2.6	0.016	11.0	0.117	0.041	6.84941	0.58870	27.0	214.6	18.4	0.002447	3.1	0.03935	0.8	0.192
26028-03B	1.2	413B	0.01710 0.00007	13434.8	247.6	1641.8	6.7	58.0	17.2	47.4	18.7	10.0	2.2	0.019	12.9	0.102	0.040	6.36146	0.42125	77.8	199.3	13.2	0.000745	21.6	0.12223	1.9	0.083
26028-03C	1.5	413B	0.01710 0.00007	30318.5	251.2	4502.6	11.7	49.4	8.3	109.6	18.8	5.5	1.9	0.051	35.4	0.086	0.015	6.37077	0.14005	94.6	199.6	4.4	0.000180	35.3	0.14854	0.9	0.022
26028-03D	2.6	413B	0.01710 0.00007	29261.1	252.0	4343.0	11.0	65.3	11.7	74.4	18.7	1.1	2.2	0.049	34.1	0.061	0.015	6.66267	0.16213	98.9	208.7	5.1	0.000037	205.2	0.14846	0.9	0.004
26028-03E	4.5	413B	0.01710 0.00007	11116.4	245.9	848.3	5.5	17.1	8.1	9.2	18.5	15.8	2.1	0.010	6.7	0.038	0.078	7.54449	0.79613	57.6	236.3	24.9	0.001421	13.5	0.07633	2.3	0.157

OL10/BOK2-4b - Aliquot #4

26028-04A	1.1	413B	0.01710 0.00007	46086.3	246.6	1181.0	6.3	28.0	9.2	-1.2	19.2	64.6	2.6	0.014	9.0	-0.003	0.048	22.69398	0.69209	58.2	710.8	21.7	0.001401	4.0	0.02563	0.8	0.095
26028-04B	1.2	413B	0.01710 0.00007	50033.6	249.2	2252.9	7.9	25.8	9.5	26.6	18.7	1.8	2.1	0.025	17.2	0.042	0.030	21.96181	0.30397	98.9	687.9	9.5	0.000037	112.7	0.04504	0.6	0.004
26028-04C	1.5	413B	0.01710 0.00007	90559.0	252.2	4301.7	10.3	48.8	10.0	29.3	18.8	2.1	2.0	0.049	32.8	0.024	0.016	20.90006	0.16128	99.3	654.6	5.1	0.000023	96.3	0.04751	0.4	0.002
26028-04D	2.6	413B	0.01710 0.00007	83596.1	248.9	3971.8	11.0	44.4	8.1	69.0	18.6	0.5	2.0	0.045	30.3	0.062	0.017	21.00418	0.17530	99.8	657.9	5.5	0.000006	395.9	0.04752	0.4	0.001
26028-04E	4.5	413B	0.01710 0.00007	29244.7	243.8	1415.7	7.2	35.9	11.3	-9.6	18.7	-2.2	2.0	0.016	10.8	-0.025	0.047	21.11764	0.46318	102.3	661.4	14.5	-0.000075	-89.6	0.04842	1.0	0.008

OL10/BOK2-4b - Aliquot #5

26028-05A	1.1	413B	0.01710 0.00007	39076.7	250.8	1739.5	7.3	28.9	8.2	15.4	19.3	89.5	2.6	0.020	8.2	0.026	0.033	7.10450	0.47196	31.6	222.6	14.8	0.002290	3.0	0.04452	0.8	0.180
26028-05B	1.2	413B	0.01710 0.00007	18491.4	244.1	2041.9	7.1	46.5	7.3	22.8	18.7	8.7	2.1	0.023	9.7	0.039	0.033	7.78321	0.32932	86.0	243.8	10.3	0.000470	24.1	0.11045	1.4	0.053
26028-05C	1.5	413B	0.01710 0.00007	62953.1	249.0	4166.9	10.6	67.3	10.1	56.5	18.6	101.4	2.6	0.047	19.7	0.048	0.016	7.84369	0.19822	51.9	245.7	6.2	0.001610	2.6	0.06621	0.5	0.128
26028-05D	2.6	413B	0.01710 0.00007	94225.4	258.1	11873.7	19.4	160.0	10.0	137.6	18.7	31.2	2.3	0.134	56.2	0.041	0.006	7.15103	0.06196	90.1	224.0	1.9	0.000331	7.3	0.12604	0.3	0.033
26028-05E	4.5	413B	0.01710 0.00007	10540.8	255.0	1301.1	6.0	41.9	9.1	18.9	18.6	1.7	2.0	0.015	6.2	0.052	0.051	7.71652	0.49588	95.3	241.7	15.5	0.000158	118.7	0.12347	2.5	0.020

OL10/BOK2-4b - Aliquot #6

26028-06A	1.1	413B	0.01710 0.00007	66697.9	253.9	629.0	4.4	60.4	19.3	15.1	19.2	66.2	2.7	0.007	7.6	0.071	0.091	74.63070	1.42325	70.4	2336.5	44.5	0.000992	4.0	0.00943	0.8	0.046
26028-06B	1.2	413B	0.01710 0.00007	65648.2	260.7	1019.0	5.0	26.3	9.3	-11.9	18.6	-3.9	2.0	0.012	12.3	-0.042	0.065	65.56093	0.71209	101.8	2052.7	22.3	-0.000060	-50.4	0.01553	0.6	0.005
26028-06C	1.5	413B	0.01710 0.00007	147287.6	265.8	2304.5	7.3	67.4	18.6	17.1	18.6	-1.1	2.1	0.026	27.9	0.026	0.029	64.03645	0.36130	100.2	2005.0	11.3	-0.000007	-199.8	0.01565	0.4	0.000
26028-06D	2.6	413B	0.01710 0.00007	227343.3	268.8	3509.9	10.3	54.0	11.3	38.4	18.6	5.2	2.2														

TABLE DR1-3 - SCIH analytical data

Lab ID#	Watts	Irrad.	<i>J</i>	Relative Isotopic Abundances												Derived Results								Inverse Isochron Data				
				⁴⁰ Ar			³⁹ Ar			³⁸ Ar			³⁷ Ar			³⁶ Ar			³⁹ Ar Mol × 10 ⁻¹⁵	³⁹ Ar % of total	Ca/K	⁴⁰ Ar / ³⁹ Ar		% ⁴⁰ Ar*	Age (Ma)	³⁶ Ar / ⁴⁰ Ar	³⁹ Ar / ⁴⁰ Ar	³⁶ Ar / ³⁹ Ar
(X 10 ⁻³) ± 1σ	±1σ	±1σ	±1σ	±1σ	±1σ	±1σ	±1σ	±1σ	±1σ	±1σ	±1σ	±1σ	±1σ	±1σ	±1σ	±1σ	±1σ	±1σ	±1σ	±1σ	±1σ	±1σ	±1σ	±1σ	±1σ	Er. Corr.		
26028-07A	1.1	413B	0.01710	0.00007	37851.5	253.6	766.0	4.9	27.9	8.7	27.5	19.3	109.9	2.7	0.009	13.5	0.106	0.075	6.59749	1.08790	13.4	206.7	34.1	0.002902	2.5	0.02024	0.9	0.194
26028-07B	1.2	413B	0.01710	0.00007	7431.0	248.3	1059.4	5.7	7.9	11.1	37.5	18.5	0.3	2.1	0.012	18.6	0.126	0.062	6.93900	0.64939	98.9	217.4	20.3	0.000035	818.6	0.14260	3.4	0.004
26028-07C	1.5	413B	0.01710	0.00007	19641.3	249.9	3059.2	8.9	39.4	12.4	118.2	18.6	4.5	2.0	0.035	53.8	0.138	0.022	5.98510	0.21231	93.2	187.5	6.7	0.000226	45.0	0.15579	1.3	0.028
26028-07D	2.6	413B	0.01710	0.00007	4064.1	249.5	580.0	3.9	0.6	9.7	8.3	18.5	0.9	2.0	0.007	10.2	0.051	0.114	6.53617	1.12338	93.3	204.8	35.2	0.000225	220.9	0.14274	6.2	0.028
26028-07E	4.5	413B	0.01710	0.00007	2543.4	248.4	223.6	3.0	-1.9	9.2	6.2	18.6	1.9	2.2	0.003	3.9	0.099	0.299	8.90111	3.16846	78.3	278.8	99.2	0.000728	120.4	0.08794	9.9	0.080

OL10/BOK2-4b - Aliquot #8

26028-08A	1.1	413B	0.01710	0.00007	114127.6	258.7	1335.2	6.4	55.5	6.7	14.8	19.2	89.4	2.7	0.016	15.1	0.033	0.043	65.47022	0.71140	76.6	2049.9	22.3	0.000784	3.0	0.01170	0.5	0.033
26028-08B	1.2	413B	0.01710	0.00007	90173.8	255.2	1285.1	6.8	7.8	11.5	-2.7	18.5	29.5	2.3	0.015	14.6	-0.008	0.052	63.31062	0.65514	90.2	1982.3	20.5	0.000327	7.7	0.01425	0.6	0.018
26028-08C	1.5	413B	0.01710	0.00007	160084.6	259.3	2186.9	9.0	43.6	9.8	19.1	18.5	61.7	2.5	0.025	24.8	0.031	0.030	64.76079	0.44807	88.5	2027.7	14.0	0.000386	4.0	0.01366	0.4	0.016
26028-08D	2.6	413B	0.01710	0.00007	256668.5	279.3	3845.0	11.9	0.9	21.4	9.2	19.3	31.3	3.4	0.025	43.6	0.008	0.018	64.31148	0.34027	96.4	2013.6	10.6	0.000122	11.0	0.01498	0.3	0.004
26028-08E	4.5	413B	0.01710	0.00007	10828.7	255.8	176.6	2.5	-23.3	6.9	-8.7	18.6	-1.9	2.0	0.002	2.0	-0.178	0.378	64.50351	3.76185	105.2	2019.6	117.7	-0.000174	-104.9	0.01631	2.8	0.019

OL10/BOK2-4b - Aliquot #9

26028-09A	1.1	413B	0.01710	0.00007	130065.0	252.7	1328.7	6.0	61.9	10.7	32.9	19.3	149.9	3.1	0.016	16.1	0.073	0.043	64.19343	0.78578	65.6	2009.9	24.6	0.001153	2.1	0.01022	0.5	0.038
26028-09B	1.2	413B	0.01710	0.00007	115101.3	265.9	1764.8	7.0	50.9	21.2	28.2	18.6	-0.9	2.4	0.020	21.3	0.057	0.038	65.36601	0.50159	100.2	2046.6	15.7	-0.000008	-251.1	0.01534	0.5	0.000
26028-09C	1.5	413B	0.01710	0.00007	88477.0	259.4	1385.2	5.9	7.0	9.0	30.3	18.6	-0.3	2.0	0.016	16.7	0.078	0.048	63.93105	0.53838	100.1	2001.7	16.8	-0.000004	-609.3	0.01566	0.5	0.000
26028-09D	2.6	413B	0.01710	0.00007	153991.3	260.6	2165.0	7.3	38.3	11.8	10.9	18.6	45.9	2.5	0.024	26.2	0.018	0.031	64.78079	0.42489	91.1	2028.3	13.3	0.000298	5.4	0.01406	0.4	0.015
26028-09E	4.5	413B	0.01710	0.00007	106874.8	258.7	1633.4	6.0	28.5	12.7	25.7	18.6	5.7	2.2	0.018	19.7	0.056	0.041	64.38232	0.49527	98.4	2015.8	15.5	0.000053	39.1	0.01529	0.4	0.003

OL10/BOK2-4b - Aliquot #10

26028-10A	1.1	413B	0.01710	0.00007	22529.1	247.6	885.0	5.0	32.9	10.2	-25.6	19.3	51.1	2.5	0.010	12.8	-0.087	0.065	8.19628	0.88367	32.2	256.8	27.7	0.002271	5.0	0.03929	1.2	0.197
26028-10B	1.2	413B	0.01710	0.00007	7189.4	257.4	980.5	5.7	1.7	5.1	-8.9	18.6	-0.6	2.0	0.011	14.2	-0.033	0.068	7.52103	0.67030	102.6	235.6	21.0	-0.000087	-323.1	0.13641	3.6	0.011
26028-10C	1.5	413B	0.01710	0.00007	4553.5	258.6	666.7	4.3	1.0	10.4	-2.4	18.6	-0.1	2.0	0.008	9.6	-0.013	0.100	6.86222	0.97667	100.5	215.0	30.6	-0.000017	-2625.2	0.14645	5.7	0.002
26028-10D	2.6	413B	0.01710	0.00007	20320.3	263.8	2875.2	9.6	31.7	12.6	13.5	18.5	1.1	2.0	0.032	41.6	0.016	0.023	6.94799	0.22999	98.3	217.7	7.2	0.000056	178.3	0.14153	1.3	0.007
26028-10E	4.5	413B	0.01710	0.00007	10659.3	266.6	1508.3	7.7	29.3	10.4	9.0	18.6	-1.9	2.2	0.017	21.8	0.021	0.044	7.43642	0.47776	105.2	233.0	15.0	-0.000176	-119.3	0.14153	2.6	0.021

OL11/OLT-1

26029-01A	1.1	413B	0.01710	0.00007	88664.3	255.6	410.9	3.1	72.6	13.9	27.7	19.3	277.8	3.6	0.005	0.8	0.201	0.140	13.93340	2.72131	6.5	436.4	85.2	0.003133	1.3	0.00463	0.8	0.078
26029-01B	1.2	413B	0.01710	0.00007	20935.3	228.3	1023.9	5.3	14.8	7.9	44.9	18.7	56.9	2.5	0.012	2.1	0.152	0.064	3.86901	0.76920	18.9	121.2	24.1	0.002716	4.6	0.04892	1.2	0.215
26029-01C	1.3	413B	0.01710	0.00007	6380.1	227.4	909.8	5.2	19.6	5.6	26.0	18.7	5.9	2.1	0.010	1.9	0.099	0.071	5.06842	0.72828	72.3	158.8	22.8	0.000928	35.4	0.14263	3.6	0.100
26029-01D	1.4	413B	0.01710	0.00007	7793.8	228.6	1128.1	5.9	30.7	10.9	15.2	18.7	10.1	2.0	0.013	2.3	0.046	0.058	4.23895	0.57848	61.4	132.8	18.1	0.001294	20.5	0.14477	3.0	0.141
26029-01E	1.6	413B	0.01710	0.00007	12208.1	229.5	2058.8	7.4	40.0	7.2	56.5	18.7	19.0	2.3	0.023	4.2	0.095	0.032	3.17048	0.35804	53.5	99.3	11.2	0.001558	12.5	0.16868	1.9</td	

TABLE DR1-3 - SCIH analytical data

Lab ID#	Watts	Irrad.	J	Relative Isotopic Abundances												Derived Results								Inverse Isochron Data			
				^{40}Ar			^{39}Ar			^{38}Ar			^{37}Ar			^{36}Ar			^{39}Ar Mol $\times 10^{-15}$	^{39}Ar % of total	Ca/K	$^{40}\text{Ar}/^{39}\text{Ar}$	% $^{40}\text{Ar}^*$	Age (Ma)	$^{36}\text{Ar}/^{40}\text{Ar}$	$^{39}\text{Ar}/^{40}\text{Ar}$	$^{36}\text{Ar}/^{39}\text{Ar}$
				$\pm 1\sigma$				$\pm 1\sigma$				$\pm 1\sigma$						$\pm 1\sigma$		$\pm 1\sigma$		$\pm 1\sigma$		$\pm 1\sigma$			
26029-02B	1.2	413B	0.01710 0.00007	13693.1	230.8	1271.2	5.9	28.1	9.1	77.5	18.7	29.5	2.1	0.014	7.1	0.212	0.051	3.84562	0.52696	35.7	120.5	16.5	0.002154	7.3	0.09285	1.7	0.221
26029-02C	1.3	413B	0.01710 0.00007	7152.5	229.4	989.2	5.4	18.3	11.0	75.5	18.7	15.0	2.1	0.011	5.5	0.265	0.066	2.71068	0.66390	37.5	84.9	20.8	0.002094	14.1	0.13832	3.3	0.224
26029-02D	1.4	413B	0.01710 0.00007	9822.6	226.4	1242.4	5.5	49.2	9.6	83.6	18.6	16.7	2.0	0.014	6.9	0.234	0.052	3.89274	0.51279	49.2	121.9	16.1	0.001700	12.2	0.12651	2.3	0.186
26029-02E	1.6	413B	0.01710 0.00007	9379.3	230.1	1615.1	6.8	24.1	12.0	78.9	18.7	14.2	2.1	0.018	9.0	0.170	0.040	3.18539	0.41091	54.9	99.8	12.9	0.001512	14.9	0.17223	2.5	0.162
26029-02F	2	413B	0.01710 0.00007	5913.9	230.7	1529.1	6.7	45.9	20.5	81.9	18.8	0.8	2.3	0.017	8.5	0.186	0.043	3.71657	0.47234	96.1	116.4	14.8	0.000130	297.5	0.25860	3.9	0.013
26029-02G	2.5	413B	0.01710 0.00007	53000.1	234.0	5338.0	11.9	98.4	12.1	296.1	18.8	119.6	2.9	0.060	29.6	0.193	0.012	3.24532	0.17060	32.7	101.7	5.3	0.002255	2.5	0.10073	0.5	0.158
26029-02H	3	413B	0.01710 0.00007	14817.5	232.0	3732.2	9.9	62.2	9.0	154.1	18.7	10.7	1.9	0.042	20.7	0.144	0.018	3.11687	0.16385	78.5	97.6	5.1	0.000719	17.8	0.25193	1.6	0.087
26029-02I	4	413B	0.01710 0.00007	9178.9	229.7	1094.8	5.6	11.5	8.6	84.2	18.7	21.2	2.1	0.012	6.1	0.268	0.059	2.60252	0.61659	31.0	81.5	19.3	0.002310	10.3	0.11929	2.6	0.237
26029-02J	5	413B	0.01710 0.00007	2252.7	227.9	507.8	3.3	49.6	13.1	8.8	18.7	1.3	2.0	0.006	2.8	0.060	0.129	3.64803	1.23327	82.2	114.3	38.6	0.000595	146.2	0.22546	10.1	0.069

OL11/OLT-1 - Aliquot #3

26029-03A	1.1	413B	0.01710 0.00007	59547.7	263.9	1046.7	5.4	57.0	9.9	54.1	19.3	98.0	2.6	0.012	2.9	0.154	0.055	28.95154	0.79941	50.9	906.8	25.0	0.001645	2.7	0.01758	0.7	0.108
26029-03B	1.2	413B	0.01710 0.00007	8416.5	229.4	1471.5	6.4	43.2	13.9	45.6	18.8	8.2	1.9	0.017	4.0	0.108	0.045	4.06784	0.41625	71.1	127.4	13.0	0.000967	23.5	0.17487	2.8	0.114
26029-03C	1.4	413B	0.01710 0.00007	11898.4	231.3	2320.4	8.7	11.7	10.7	50.1	18.9	9.4	2.1	0.026	6.4	0.075	0.028	3.92223	0.28986	76.5	122.9	9.1	0.000787	22.7	0.19506	2.0	0.084
26029-03D	1.6	413B	0.01710 0.00007	14973.5	236.5	3190.7	10.7	46.1	8.4	73.0	18.8	14.9	2.0	0.036	8.8	0.079	0.021	3.30260	0.20329	70.4	103.5	6.4	0.000992	13.7	0.21314	1.6	0.113
26029-03E	2	413B	0.01710 0.00007	17503.6	240.3	3607.8	9.8	20.7	12.4	127.7	18.7	7.0	2.2	0.041	9.9	0.123	0.018	4.27501	0.19479	88.1	133.9	6.1	0.000397	31.8	0.20616	1.4	0.042
26029-03F	2.5	413B	0.01710 0.00007	25519.9	255.4	7165.6	14.8	71.1	11.4	188.5	18.8	6.9	2.1	0.081	19.7	0.092	0.009	3.27847	0.09564	92.1	102.7	3.0	0.000265	31.4	0.28085	1.0	0.031
26029-03G	3	413B	0.01710 0.00007	12849.7	257.6	3389.0	10.0	20.1	5.8	103.7	18.7	7.5	2.2	0.038	9.3	0.107	0.019	3.13562	0.21113	82.7	98.2	6.6	0.000579	30.1	0.26380	2.0	0.066
26029-03H	4	413B	0.01710 0.00007	33209.8	264.3	10429.4	16.4	101.4	13.0	308.1	18.7	-1.9	2.0	0.118	28.7	0.103	0.006	3.24125	0.06397	101.8	101.5	2.0	-0.000061	-101.2	0.31413	0.8	0.008
26029-03I	5	413B	0.01710 0.00007	13117.9	266.3	3770.9	9.9	29.4	8.8	120.4	18.7	3.8	2.2	0.043	10.4	0.111	0.017	3.18297	0.19057	91.5	99.7	6.0	0.000284	60.0	0.28753	2.0	0.034

OL11/OLT-1 - Aliquot #4

26029-04A	1.1	413B	0.01710 0.00007	12486.8	263.1	996.8	5.3	12.6	7.1	58.6	19.3	31.3	2.6	0.012	15.7	0.175	0.058	3.15779	0.80906	25.2	98.9	25.3	0.002505	8.4	0.07984	2.2	0.242
26029-04B	1.2	413B	0.01710 0.00007	5124.9	267.3	836.0	4.8	-4.7	11.4	60.2	18.8	9.6	2.1	0.009	13.1	0.252	0.079	2.70297	0.82925	44.1	84.7	26.0	0.001872	22.9	0.16316	5.2	0.226
26029-04C	1.4	413B	0.01710 0.00007	1407.0	265.6	500.8	4.2	-20.2	9.1	1.9	18.7	1.0	2.0	0.006	7.9	0.013	0.131	2.23110	1.30472	79.4	69.9	40.9	0.000689	207.2	0.35602	18.9	0.091
26029-04D	1.6	413B	0.01710 0.00007	1546.3	263.4	490.3	3.3	-16.0	11.5	44.4	18.7	4.2	2.1	0.006	7.7	0.317	0.134	2.92619	1.39757	92.8	91.7	43.8	0.000241	568.8	0.31715	17.1	0.030
26029-04E	2	413B	0.01710 0.00007	757.0	263.2	344.8	3.4	-2.5	8.0	7.3	18.7	-1.4	2.2	0.004	5.4	0.073	0.190	3.39232	2.01582	154.6	106.3	63.1	-0.001828	-159.6	0.45563	34.8	0.218
26029-04F	2.5	413B	0.01710 0.00007	31462.0	263.7	1591.8	7.1	14.0	9.2	80.2	18.7	84.9	3.1	0.018	25.0	0.176	0.041	3.84545	0.60338	19.5	120.5	18.9	0.002698	3.7	0.05060	0.9	0.198
26029-04G	3	413B	0.01710 0.00007	3174.8	260.0	1100.1	5.4	1.0	6.1	78.4	18.7	-4.0	2.0	0.012	17.3	0.249	0.060	3.98800	0.59620	138.2	124.9	18.7	-0.001280	-50.3	0.34657	8.2	0.163
26029-04H	4	413B	0.01710 0.00007	999.0	256.4	296.0	3.5	-5.3	7.2	-31.5	18.7	-5.3	2.1	0.003	4.6	-0.374	0.222	8.73510	2.27642	258.9	273.6	71.3	-0.005322	-46.9	0.29640	25.7	0.547
26029-04I	5	413B	0.01710 0.00007	532.9	253.7	211.1	3.0	2.3	8.5	-12.7	18.7	-1.2	2.4	0.002	3.3	-0.212	0.311	4.15937	3.62583	164.8	130.3	113.6	-0.002172	-214.4	0.39633	47.6	0.222

OL11/OLT-1 - Aliquot #5

26029-05A	1.1	413B	0.01710 0.00007	121
-----------	-----	------	-----------------	-----

TABLE DR1-3 - SCIH analytical data

Lab ID#	Watts	Irrad.	<i>J</i> (X 10 ⁻³) ± 1σ	Relative Isotopic Abundances								Derived Results								Inverse Isochron Data							
				⁴⁰ Ar ±1σ	³⁹ Ar ±1σ	³⁸ Ar ±1σ	³⁷ Ar ±1σ	³⁶ Ar ±1σ	³⁹ Ar Mol ∞ 10 ⁻¹⁵	³⁹ Ar % of total	Ca/K ±1σ	⁴⁰ Ar/ ³⁹ Ar ±1σ	% ⁴⁰ Ar*	Age (Ma) ±1σ	³⁶ Ar/ ⁴⁰ Ar ±%1σ	³⁹ Ar/ ⁴⁰ Ar ±%1σ	³⁶ Ar/ ³⁹ Ar Er. Corr.										
<i>OL11/OLT-1 - Aliquot #6</i>																											
26029-06A	1.1	413B	0.01710 0.00007	18206.8	262.8	441.5	3.5	9.6	10.9	56.7	19.2	55.4	2.7	0.005	7.7	0.383	0.130	3.78694	1.89206	9.2	118.6	59.3	0.003042	5.0	0.02425	1.6	0.253
26029-06B	1.2	413B	0.01710 0.00007	4840.4	268.8	440.0	3.4	4.4	11.9	45.9	18.8	10.9	2.1	0.005	7.7	0.367	0.150	3.58691	1.55191	32.6	112.4	48.6	0.002257	20.0	0.09091	5.6	0.275
26029-06C	1.4	413B	0.01710 0.00007	13735.8	269.5	766.5	5.1	-39.5	17.1	65.2	18.7	39.6	2.5	0.009	13.4	0.299	0.086	2.49737	1.01755	13.9	78.2	31.9	0.002883	6.5	0.05581	2.1	0.286
26029-06D	1.6	413B	0.01710 0.00007	6572.0	259.2	460.8	4.2	-5.8	12.8	35.7	18.6	17.7	2.0	0.005	8.1	0.272	0.142	2.78406	1.40194	19.5	87.2	43.9	0.002696	11.9	0.07012	4.0	0.324
26029-06E	2	413B	0.01710 0.00007	3961.7	253.7	460.6	3.8	1.9	9.3	13.6	18.6	6.6	2.2	0.005	8.1	0.104	0.142	4.30473	1.55010	50.1	134.9	48.6	0.001673	34.3	0.11630	6.5	0.185
26029-06F	2.5	413B	0.01710 0.00007	10686.2	250.6	1379.5	5.8	4.6	11.0	125.8	18.7	19.9	2.1	0.016	24.2	0.321	0.048	3.44260	0.49793	44.4	107.8	15.6	0.001861	11.0	0.12911	2.4	0.210
26029-06G	3	413B	0.01710 0.00007	17076.4	252.5	954.5	4.9	47.2	15.0	70.8	18.7	38.9	2.2	0.011	16.7	0.261	0.069	5.73576	0.74365	32.1	179.7	23.3	0.002275	5.9	0.05591	1.6	0.237
26029-06H	4	413B	0.01710 0.00007	9205.3	252.7	400.9	3.7	-19.3	16.1	36.3	18.6	27.3	2.5	0.005	7.0	0.320	0.164	2.67533	1.99781	11.7	83.8	62.6	0.002959	9.7	0.04356	2.9	0.267
26029-06I	5	413B	0.01710 0.00007	3652.8	252.1	401.8	3.5	-7.8	9.6	62.6	18.7	7.4	2.0	0.005	7.0	0.550	0.164	3.60587	1.63841	39.7	113.0	51.3	0.002021	28.4	0.11000	7.0	0.241
<i>OL11/OLT-1 - Aliquot #7</i>																											
26029-07A	1.1	413B	0.01710 0.00007	77753.5	260.9	1504.7	6.3	51.5	7.9	234.0	19.3	220.1	3.4	0.018	16.2	0.465	0.038	8.02032	0.69528	15.5	251.2	21.8	0.002830	1.6	0.01935	0.5	0.135
26029-07B	1.2	413B	0.01710 0.00007	29502.1	252.7	1312.9	5.7	24.1	7.5	166.9	18.7	67.5	2.4	0.015	14.1	0.448	0.050	7.14966	0.58486	31.8	224.0	18.3	0.002284	3.7	0.04450	1.0	0.206
26029-07C	1.6	413B	0.01710 0.00007	23304.0	252.0	1266.2	6.1	30.4	8.8	198.9	18.7	51.6	2.4	0.014	13.6	0.554	0.052	6.26481	0.60102	34.0	196.2	18.8	0.002209	4.8	0.05434	1.2	0.206
26029-07D	2	413B	0.01710 0.00007	18488.4	249.6	2838.0	9.4	38.6	12.2	337.2	18.8	24.6	2.5	0.032	30.5	0.419	0.023	3.94546	0.27750	60.6	123.6	8.7	0.001321	10.3	0.15351	1.4	0.127
26029-07E	2.5	413B	0.01710 0.00007	11681.8	246.9	1339.4	6.4	22.5	7.0	152.4	18.7	21.6	2.2	0.015	14.4	0.402	0.049	3.92594	0.52882	45.0	123.0	16.6	0.001842	10.5	0.11467	2.2	0.196
26029-07F	3.7718	413B	0.01710 0.00007	8394.0	243.5	1045.5	5.5	-2.1	9.9	112.8	18.8	15.5	2.5	0.012	11.2	0.381	0.064	3.61702	0.73927	45.1	113.3	23.2	0.001840	16.2	0.12457	2.9	0.177
<i>OL11/OLT-1 - Aliquot #8</i>																											
26029-08A	1.1	413B	0.01710 0.00007	20763.7	255.6	876.2	4.9	5.0	7.3	70.1	19.3	47.5	2.4	0.010	12.6	0.239	0.066	7.51313	0.88297	31.7	235.4	27.7	0.002287	5.3	0.04220	1.4	0.212
26029-08B	1.2	413B	0.01710 0.00007	4393.3	247.0	907.9	5.0	54.5	12.6	6.8	18.7	3.1	2.0	0.010	13.0	0.026	0.073	3.83573	0.71792	79.3	120.2	22.5	0.000694	66.5	0.20671	5.6	0.084
26029-08C	1.6	413B	0.01710 0.00007	4746.1	248.9	1008.7	5.3	4.8	6.1	52.5	18.6	5.7	2.1	0.011	14.5	0.184	0.065	3.03068	0.66630	64.4	94.9	20.9	0.001192	37.3	0.21258	5.3	0.140
26029-08D	2	413B	0.01710 0.00007	147.8	250.6	403.8	3.2	22.3	13.0	18.5	18.7	-4.5	2.1	0.005	5.8	0.162	0.164	3.73644	1.66817	1021.6	117.0	52.3	-0.030869	-175.8	2.73418	169.7	0.965
26029-08E	2.5	413B	0.01710 0.00007	3386.5	250.3	1188.1	5.2	9.6	6.8	51.3	18.7	-2.4	2.0	0.013	17.0	0.153	0.056	3.46013	0.55156	121.4	108.4	17.3	-0.000718	-83.8	0.35092	7.4	0.088
26029-08F	5	413B	0.01710 0.00007	8158.9	243.4	2591.5	8.3	37.4	11.0	133.6	18.7	1.1	2.2	0.029	37.1	0.182	0.026	3.03312	0.26588	96.4	95.0	8.3	0.000122	217.2	0.31770	3.0	0.014
<i>OL11/OLT-1 - Aliquot #9</i>																											
26029-09A	1.1	413B	0.01710 0.00007	10218.9	251.7	745.4	4.7	40.8	10.7	38.4	19.3	21.8	2.1	0.009	12.2	0.154	0.077	4.99569	0.91597	36.4	156.5	28.7	0.002129	10.1	0.07295	2.5	0.237
26029-09B	1.2	413B	0.01710 0.00007	6390.0	235.4	760.2	4.3	9.3	6.4	4.2	18.8	14.6	2.2	0.009	12.4	0.019	0.088	2.65372	0.90156	31.6	83.1	28.2	0.002292	15.2	0.11899	3.7	0.240
26029-09C	1.6	413B	0.01710 0.00007	2403.7	226.8	449.7	3.6	17.8	9.0	15.5	18.7	4.1	2.2	0.005	7.3	0.122	0.148	2.59880	1.51640	48.6	81.4	47.5	0.001721	52.9	0.18713	9.5	0.178
26029-09D	2	413B	0.01710 0.00007	2087.2	226.7	407.4	3.6	1.5	7.7	33.2	18.6	-0.6	2.2	0.005	6.7	0.289	0.162	5.56393	1.72072	108.6	174.3	53.9	-0.000289	-368.7	0.19523	10.9	0.029
26029-09E	2.5	413B	0.01710 0.00007	10594.9	229.2	2393.5	8.5	58.2	14.9	124.9	18.8	10.6	2.0	0.027	39.1	0.185	0.028	3.10799	0.27026	70.2	97.4	8.5	0.000997	19.3	0.22595	2.2	0.111
26029-09F	5	413B	0.01710 0.00007	4817.5	232.5	1367.4	6.3	-8.8	9.1	46.4	18.6	-2.6	1.9	0.015	22.3	0.120	0.048	4.08497	0.44459	116.0	128.0	13.9	-0.000535	-73.1	0.28390	4.8	0.066

Notes:

Lab ID# in bold are steps incorporated into an age plateau.

TABLE DR1-4 - SCIH Isochron Results

Run ID	Integrated Gas Results						Plateau / Isochron Results									% ^{39}Ar in Plateau
	$^{40}\text{Ar}^*/^{39}\text{K}$	$\pm^{40}\text{Ar}^*/^{39}\text{K}$	Age	\pm Age (1 σ)	Moles ^{39}Ar	Ca/K	\pm Ca/K (1 σ)	Age (ka)	\pm Age (1 σ)	$(^{40}\text{Ar}/^{36}\text{Ar})_{\text{tr}}$	$\pm (^{40}\text{Ar}/^{36}\text{Ar})_{\text{tr}}$	MSWD	Probability	n Included	n total	
OL04/G-4p (Irradiation 416a, J = 0.0001432 ± 0.00000028)																
26074-01	0.8632	0.0189	226.2	5.0	1.60E-15	0.035	0.031	223.9	3.4	331.4	37.3	0.32	0.86	6	6	100
26074-02	0.9519	0.0231	249.5	6.0	1.30E-15	0.005	0.008	256.1	4.3	263.9	28.5	0.59	0.67	6	6	100
26074-03	1.2531	0.0306	328.4	8.0	8.25E-16	No plateaus										6
26074-04	0.8240	0.0128	215.9	3.3	2.09E-15	-0.016	0.055	217.4	1.9	230.0	60.7	0.96	0.41	5	5	100
26074-05	0.9925	0.0377	260.1	9.9	7.62E-16	0.004	0.035	226.1	9.1	343.8	127.3	0.86	0.42	4	6	95.4
26074-06	0.9224	0.0290	241.7	7.6	9.93E-16	0.098	0.017	238.8	7.9	439.8	194.9	0.38	0.82	6	6	100
26074-07	0.8888	0.0329	232.9	8.6	8.97E-16	-0.013	0.049	232.4	8.0	385.3	170.7	0.33	0.86	6	6	100
26074-08	0.8751	0.0178	229.3	4.7	1.63E-15	-0.013	0.010	228.9	13.0	1303.9	1879.7	0.86	0.42	4	6	99.2
26074-09	0.8703	0.0170	228.1	4.5	1.78E-15	0.014	0.008	224.2	7.6	308.9	35.1	0.52	0.72	6	6	100
26074-10	0.8583	0.0231	224.9	6.1	1.31E-15	0.033	0.007	223.6	4.6	340.7	70.6	0.23	0.92	6	6	100
26074-11	0.8092	0.0129	212.1	3.4	1.39E-15	-0.006	0.075	224.9	3.5	237.6	32.3	0.72	0.61	7	7	100
26074-12	0.9561	0.0176	250.5	4.6	8.90E-16	No plateaus										7
26074-13	0.8291	0.0140	217.3	3.7	1.25E-15	-0.020	6.798	219.8	3.2	293.7	10.2	0.64	0.63	6	7	99.7
26074-14	0.8377	0.0137	219.5	3.6	1.29E-15	-1.54257	141.79733	227.3	4.3	274.9	13.5	1.34	0.25	7	7	100
Weighted Mean of included analyses ($\pm 2 \sigma$):										223.6	3.3					
OL10/BOK2-4b (Irradiation 413b, J = 0.00001712 ± 0.00000007)																
26028-01	16.6148	0.4021	520.0	13.0	5.56E-17	0.013	0.122	518.9	12.0	299.7	6.9	0.22	0.93	6	6	100
26028-02	8.0834	0.1829	253.0	6.0	9.17E-17	-0.014	0.019	247.4	5.2	305.1	15.4	1.67	0.17	5	5	100
26028-03	6.5997	0.1381	207.0	4.0	1.44E-16	0.073	0.021	203.3	3.5	306.5	10.3	1.12	0.34	5	5	100
26028-04	21.2998	0.1610	667.0	5.0	1.35E-16	0.052	0.045	657.1	2.9	196.7	177.9	0.14	0.70	3	3	74
26028-05	7.3799	0.0906	231.0	3.0	2.19E-16	No plateau										5
26028-06	65.2724	0.3733	2044.0	12.0	7.48E-17	0.017	0.341	2015	10	323.5	254.6	2.30	0.10	4	4	92
26028-07	6.4157	0.3035	201.0	10.0	6.45E-17	0.111	0.059	191.1	6.3	302.5	7.9	0.98	0.40	5	5	100
26028-08	64.4929	0.4003	2019.0	13.0	8.16E-17	0.032	0.215	2007	20	311.1	33.8	1.55	0.21	4	4	81
26028-09	64.5936	0.3793	2022.0	12.0	5.85E-17	0.038	0.038	2024.6	9.9	295.6	8.9	1.46	0.23	5	5	100
26028-10	7.2876	0.2474	228.0	8.0	7.84E-17	0.044	0.135	221.6	6.4	318.1	16.6	0.45	0.72	5	5	100
Weighted Mean of included analyses ($\pm 2 \sigma$):										200	11					
OL11/OLT-1 (Irradiation 413b, J = 0.00001712 ± 0.00000007)																
26029-01	3.3111	0.0452	103.7	1.4	4.94E-16	0.117	0.018	106.9	2.8	313.3	19.0	1.75	0.13	6	9	51
26029-02	3.8228	0.1349	120.0	4.0	1.96E-16	0.175	0.033	99.2	5.3	304.4	11.3	0.87	0.53	9	9	96
26029-03	4.1565	0.0651	130.0	2.0	2.79E-16	0.101	0.005	101.6	1.7	290.6	70.3	0.24	0.79	4	4	68
26029-04	3.6274	0.3772	114.0	12.0	7.22E-17	0.096	0.586	109	13	301.1	13.9	0.82	0.57	9	9	100
26029-05	3.1564	0.1811	99.0	6.0	1.41E-16	0.186	0.047	100.1	4.2	291.6	23.7	0.67	0.70	9	9	100
26029-06	3.7095	0.4123	116.0	13.0	6.45E-17	0.272	0.083	111	18	308.5	17.7	1.37	0.21	9	9	100
26029-07	5.3300	0.2307	167.0	7.0	8.81E-17	0.407	0.023	127	24	285.9	70.0	0.14	0.71	3	3	56
26029-08	3.8126	0.2628	119.0	8.0	7.91E-17	0.094	0.142	98.1	8.2	345.7	125.9	0.42	0.74	5	5	87
26029-09	3.6249	0.2915	114.0	9.0	6.94E-17	0.083	0.202	104	12	325.5	45.9	2.06	0.08	6	6	100
Weighted Mean of included analyses ($\pm 2 \sigma$):										102.5	2.7					

Note: Bold Run ID denotes analysis included in the final weighted mean age.

TABLE DR2. OLTULELEI FM. LITHOFACIES AND INFERRED DEPOSITIONAL ENVIRONMENTS					
Lithofacies #	Lithology	Color	Description	Inferred Depositional Environment	Member(s)
1	Conglomerate	Brown, Gray	Boulder conglomerate with tuffaceous silt to sand matrix, matrix supported, boulders up to 3 m diameter. Forms linear bars in south western Locality OLT, caps hills in Localities A and C (south) and Locality B.	Catastrophic flood event(s)	Tinga
2	Pumice Gravel	Gray, Brown, Orange	Gravel, clast- to matrix supported pumice lapilli, usually rounded, 1-3 cm diameter, secondary amounts of silt and sand , pumices can be gray, white, orange, black; usually consistent within a bed. Occurs in channels and as widespread sheet deposits.	Fluvial and overbank, including filling of incised valleys.	Olkesiteli, Oltepesi, Tinga
3	Silty and Sandy Tuff	Light to Dark Gray	Variably mixed with silts and fine sands, may have dispersed pumices, vertical pedogenic cracking, root traces and CaCO ₃ rhyzoliths, locally abundant platey CaCO ₃ , in situ SiO ₂ stem casts.	Fluvial overbank, lake margin to lacustrine.	Olkesiteli, Oltepesi
4	Gravelly Sand	Gray, Buff	Coarse to medium-grained, with variable amounts and sizes of gravel, poor sorting, usually matrix supported, with lithic clasts (basalt, trachyte, and other volcanics), reworked CaCO ₃ , diatomite and silt intraclasts, may include reworked SiO ₂ plant debris, red silt clasts, pumices - dispersed or abundant locally. Usually fines upward.	Fluvial channel	Olkesiteli, Oltepesi
5	Gravelly Sandy Silt	Orange, light brown	Poorly sorted, with mix of gravel, sand and silt, often with abundant CaCO ₃ rhyzoliths and nodules, occasional pumice, lithics, generally lacking internal structures.	Fluvial channel and valley fills, bioturbated	Oltepesi
6	Sand	Gray, yellow-gray	Relatively well-sorted, medium to fine-grained sand, may be laminated or cross-stratified.	Fluvial, eolian	Oltepesi
7	Sandy Silt	Yellow, light brown, gray	Moderately sorted silts with minor sand, homogeneous, often pedogenically modified with clay-lined root traces and burrows, MnO mottling, CaCO ₃ nodules; may have SiO ₂ rhyzoliths and fragmented white plant stem debris, silt clasts, dispersed pumice, patches of red to orange baked sediment.	Fluvial overbank, paleosol	Olkesiteli
10	Silt	Yellow, orange, light brown	Homogeneous, moderate to well-sorted, often pedogenically modified with CaCO ₃ rhyzoliths and nodules, clay-lined root traces and burrows, MnO mottling, CaCO ₃ nodules.	Floodplain, paleosol	Oltepesi
11	Clayey Silt	Brown, orange, green	Relatively homogeneous, may have minor sand and grit, usually pedogenically modified with vertical cracking structures, CaCO ₃ nodules and rhyzoliths.	Floodplain, paleosol	Olkesiteli, Oltepesi
12	Gravelly Silty Clay	Red, brown	Non-homogenous mix of clay, lithic gravel, with silt and sand, pedogenically modified with CaCO ₃ nodules and rhyzoliths, may have vertisol structure.	Accretionary paleosol	Olkesiteli (Locality G)
13	Diatomaceous Silt	White, yellow	Bedded to massive silts with varying amounts of diatoms, may have volcaniclastics including pumice, secondary CaCO ₃ rhyzoliths and nodules, tufa structures. Rare beds of relatively pure diatomite.	Lake or wetland	Olkesiteli, Oltepesi, Tinga
14	Carbonate	White, light gray	CaCO ₃ , hard, nodular or platey beds, may have rhyzoliths, occasionally includes SiO ₂ (chert).	Paleosol B horizon, spring, wetlands, lake	Olkesiteli

SUPPLEMENTAL TEXT DR3

Detailed Stratigraphy of the Oltulelei Formation

Documentation of the Oltulelei (OL) Formation required 15 years of logging sections across the basin, and these logs provide the foundation for synthesizing the geological history represented in the main text, especially Text Figures 4, 6, 8 and 9. We present the primary stratigraphic data in the three panel diagrams for the main Olorgesailie Basin localities where the OL Fm. occurs, Localities B, OLT, and G. Abbreviations and conventions for labeling the sections are shown in Text Table 2, and detailed description of the depositional phases in each Locality are given below. Each section log was described in the field by AKB and then entered into the stratigraphic drafting program PsiCat (<http://portal.chronos.org/psicat-site/>) to standardize lithological descriptions and symbols. Lateral tracing of stratigraphic boundaries and matching of lithofacies provide the basis for correlations between sections. $^{39}\text{Ar}/^{40}\text{Ar}$ dates reported in this paper are shown on the diagrams and based on Text Table 1; in-progress geochronological work by AD will further test and refine these correlations.

The vertical positions of the sections relative to one another are based in part on lithological unit boundaries and also on topographic relationships. The complex cut and fill cycles of multiple channels are reflected in the highly variable lateral relationships of the different units and documented channel boundaries. Considerable channel erosion and deposition was going on in a relatively small area in geologically short periods of time, especially in Locality B. Most components of the depositional architecture of the Oltulelei Formation represented in the panel diagrams are secure, but some remain working hypotheses subject to further testing.

Oltulelei Fm. Depositional Phases

The different lithological units within each member are organized into a succession of depositional phases for each of the four localities (B, C, G, OLT). Some of these can be correlated using lithological similarities and geochronology, but because of the disjunct outcrops and lateral variability of the Oltulelei Fm., it is important to describe the stratigraphy of each locality separately. Defining characteristics of the Oltulelei Fm. deposits are well-represented in Locality B but important variations occur in Localities C, OLT, and G (Text Fig. 4, DR3A–DR3C). Descriptions of lithofacies and stratigraphic relationships for each member are based primarily on Locality B outcrops, where all three members occur in clear stratigraphic succession. From this evidence, we infer successive depositional phases, designating these as Phase B-1, etc. (abbreviated as B-1, B-2, etc.). Following descriptions of each Locality B depositional phase, we present inferred correlative phases in Localities C, OLT and G, building toward discussion of how all of these depositional units are assembled into the Oltulelei Fm. Text Figure 4 represents a summary of the depositional phases and their spatial and temporal relationships, based on stratigraphic sections and other information in Figs. DR3A–DR3C.

Olkesiteti (OK) Member

The deposits assigned to the OK Mb. in northern Locality B are a complex of superimposed and cross-cutting channels that can be organized into three distinct phases

involving erosion followed by filling of the channeled areas and development of associated floodplain facies. This sequence is capped by a fourth phase with a laterally extensive pumice conglomerate, which is one of the Oltulelei Tuffs based both on lithology and radiometric age.

Phase B-1

The earliest deposits of the OK Mb. occur in Phase B-1 as coarse, volcanic-sourced gravels that line the bottom of a paleo-channel exposed in the vicinity of archaeological sites BOK-1 and BOK-3 (Text Fig. 4, DR3A) (Brooks et al. 2018). These sediments form the base of section B08–01 and are exposed in the modern cut-bank of the Oltulelei River at its junction with the Ol Keju Nyiro River. This paleo-channel was directed toward the west and north-west, and the gravels are thickest just south of section B10–01+B08–06 (BOK-1), indicating the local channel axis and a likely place of convergence, with tributaries feeding in from the south and north and exiting westward through an early version of the Ol Keju Nyiro gorge. The channel was at least 50 m wide and up to ~3 m deep, with irregular basal topography on eroded OG Mb. 9 (Text Fig. 4). There are no pumices in the gravels of this channel phase. Yellow, pedogenically modified silts with occasional pumices, dark MnO mottles, and patches of reddened, baked silt occur in the upper part of Phase B-1 and represent the floodplain deposits of this channel system.

Phase G-1

In Locality G, the basal exposure of the OK Mb. (Phase G-1) is a red, calcareous, pedogenically modified gravelly clay with interbedded tufa and diatomaceous silts, deposited on the volcanic basement (Text Figs. 3, 5A, DR3C). G-1 contains archaeological materials at multiple stratigraphic levels within the red paleosol (archaeological site GOK-1; Brooks et al. 2018). The age of the ~5 m thick red paleosol is currently unknown; it may or may not be contemporaneous with B-1 but likely represents considerable time, given the thickness, accretionary structure, well-developed pedogenic fabric and abundant carbonate. Carbonate tufa deposits are associated with the lower parts of the red paleosol (Fig. DR3C).

Phase B-2

Smaller, shallower OK Mb. channels with poorly sorted gravelly sands and silts occur above Phase B-1 and represent partial reworking of the upper part of its channel fill. Flow directions were west and southwest, based on mapping of exposed channel edges (green dashed lines, Text Fig. 6) and cross-stratification. Clastic material includes tuffaceous silt, pumice, volcanic rock fragments, and reworked diatomite from the underlying Olorgesailie (OG) Fm. Networks of silicified plant stems and roots as well as white, reworked siliceous plant debris are a distinctive component of OK Phase B-2. Radiating systems of open tubes associated with silicified plants and siliceous tufts (Text Fig. 5J), some of which occur as sloping bio-silcrete channel edges, are interpreted as spring deposits associated with the upper parts of the B-2 channel fill complex. The channel in Section B01–01B, at the eastern end of the outcrops, is lined with siliceous tufa and includes diatoms indicating fresh water ponds associated with springs (Owen et al. 2014). There is general fining upward in Phase B-2 to pedogenically modified yellow, light gray and reddish brown silts, some of which have abundant platy carbonate and rhizoliths.

Phase B-3

Renewed channel cutting was followed by deposition of OK Mb. pumice-rich gravels and sandy silts, which form distinctive, reddish-orange sediments with abundant small calcareous rhizoliths. There is little lithic gravel in this channeling phase; deposition was dominated by an influx of pumiceous gravel and finer volcaniclastics, which filled small valleys and then overtopped them, creating a relatively flat depositional plain with accretionary, carbonate-rich paleosols. Based on cross-stratification and channel margins, channel directions followed the same drainage pattern as in Phase B-2 (green dashed line, Text Fig. 6). Reworked silicified plant fragments are locally common but there is no evidence for primary spring tufas comparable to those in Phase B-2.

The local complexity of OK fluvial deposits forming Phases B-1 to B-3 can be attributed to drainage control by the Ol Keju Nyiro gorge, which today cuts through the lavas of Mt. Olorgesailie (Text Figs. 1, 2, 6). Modern channels are spatially constrained to drain the NW corner of Locality B by the narrow outlet through the Mt. Olorgesailie volcanics (Text Figs. 1, 2), and sedimentological evidence including paleochannel directions and cross-stratification points to a similar situation in the past (Text Figs. 6, 9). This resulted in physiographic focusing of local OK Member drainages from the east and south as they converged toward this outlet, leading to multiple cut-and-fill fluvial cycles in a relatively small area. The fault on the west side of Locality B (Text Fig. 6) also likely affected local surface water availability, including springs.

Phase OLT-1

In Locality OLT, OK Mb. Phase OLT-1 deposits fill a valley eroded into the OG Fm. and include basal gravels with reworked OG Fm. clasts, sands and silts with pedogenic modification, pumice gravels, and a distinctive gray tuff that can be traced between exposures of the valley fill (Text Fig. 4, Fig. DR3b). A date of 291 ka on pumice lapilli near the base of this sequence (Text Table 1, Fig. 4) makes OLT-1 similar in age to the B-2 and B-3 deposits (Deino et al., 2018), indicating contemporaneous aggradation within what likely was the same east to west drainage system (Text Figs. 4, 6, 9; Figs. DR3B, DR3C).

Phase G-2

In Locality G, Phase G-2 consists of a ~4 m sequence of fine-grained tuffs and tuffaceous silts, diatomaceous silts, green, clay-rich paleosols, and carbonate tufas that unconformably overlie G-1 (Text Fig. 5B–D). Toward the south, these fill topographic lows on the irregular surface of the underlying red paleosol (Section G01–04). In the north, G-2 rests upon the Magadi Trachyte basement and has basal units of calcareous tufa with plant casts indicating paleo-spring deposition. Sections G05–02 and G06–03 have fine silt beds and tufas with diatoms indicating fresh to mildly saline shallow water habitats (Owen et al., 2014). The northern exposures also include reworked silicified plant stem debris, interbedded tufa deposits (Text Fig. 5D), and fine- to medium-grained, laterally continuous “plant stem” tuffs, some of which contain *in situ* silicified plant fossils in growth position (G06–08; Text Fig. 5B–B). It is likely that the G-2 sediments are at least partly contemporaneous with B-1 to B-3, based on their stratigraphic position below the Oltulelei Tuffs and evidence for an elevated water table.

Phase B-4

A single ~1.0 m thick bed of greenish volcanic sand with obsidian shards and black, angular pumice clasts capped by caliche forms Phase B-4 (Text Fig. 4). This distinctive tabular unit is exposed along the western margin of Locality B adjacent to the up-faulted ridge of

volcanic basement and extends southward for ~200 m, thinning to ~10 cm. It has been dated at 225 ka (Text Table 1), and this date plus lithological features (black pumice gravel in a greenish matrix, small angular obsidian clasts) identify it as a remnant of one of the Oltulelei Tuff sheet deposits that covered larger areas of Locality B. Additional evidence of greater extent is provided in both Localities OLT and B, where lithified blocks of this tuff were incorporated into the basal conglomerates of OT Mb. valley fills.

Phase OLT-2

In Locality OLT, the Oltulelei Tuffs consist of 5–6 m of tabular pumice gravels (Phase OLT-2a; Text Fig. 4, Fig. 5G; DR3B), which are separated by silts with weakly developed paleosols. Diatomaceous silts interfinger with and cap the tuffs toward the west side of Locality OLT, indicating wetland and shallow lacustrine conditions that suggest temporarily restricted drainage toward the west, either by sediment or movement along the Lava Peninsula fault that divides Localities OLT and C (Text Fig. 2). Phase OLT-2b is represented by a limited area of exposures where the uppermost Oltulelei Tuff occurs above a distinctive red-orange paleosol exposed on both the north and south sides of the modern Ol Keju Nyiro River valley. This paleosol includes scattered obsidian artifacts and represents temporary stabilization of the depositional plain sometime before the upper date of 190 ka on the Oltulelei Tuffs (Text Table 1; Text Fig. 4).

Phase G-3

Tabular beds of tuffaceous pumice gravel the same age as the Oltulelei Tuffs in Locality G (Phase G-3a; Text Fig. 4, Text Table 1, Fig. DR3C) are locally named the “Triple Tuffs” where there are three distinct superimposed tabular beds separated by silts with weak paleosols (Text Fig. 4, Fig. DR3C). In the vicinity of section G08–01 (Fig. DR3C), G3a deposits have south-directed, narrow incised channels filled with pumice gravels, which pass laterally (east- and southward) into channel and floodplain deposits with increased amounts of sand, silt, and weathered pumices reworked from the Oltulelei Tuffs. Toward the north, three pumice-rich units that correlate with the Triple Tuffs occur within broader channel fills (G06–08). Phase G-3b (Fig. DR3C), consists of up to 3.5 m of weathered pumices, interbedded tuff, lithic gravel, and silty sands, which we interpret as a channel deposit (possibly a mudflow) emplaced subsequent to deposition of the lower (Phase 3a) Oltulelei Tuffs.

Phase G-4

The floodplain deposits of OK Mb. Phase G-4 are characterized by carbonate-rich, well-developed clayey paleosols but also include coarse, poorly sorted lithic conglomerates and occasional tabular tuffs with white, silicified plant stems (“plant stem tuffs”). In the southern part of the outcrop area, pumice conglomerates represent continuing influx of the Oltulelei Tuffs. The uppermost of these occurs at the base of a channel deposit with volcanic cobbles and boulders, representing an influx of coarse alluvium likely derived from the slopes of Mt. Olorgesailie to the east. Paleosols include varying densities of carbonate nodules, root casts, and sediments with relict bedding structures.

Clastic Dikes

Vertical crack fills up to 10 m in depth are an additional feature of the OK Mb. These occur locally in the eastern outcrop areas (Localities OLT, B) and cut through strata underlying

the Oltulelei Tuffs (OK Mb. and OG Fm.). The cracks are filled with orange sandy silt and gray to black pumices and are interpreted as clastic dikes. They are more common near faults in the OK Mb. and most do not extend upward through the OT Mb. Pumices from one of these dikes in Locality B have a variety of ages, with a youngest component at ~200 ka (Text Table 1, Fig. DR3A), suggesting that some of the dikes are associated with the vulcanism that generated the Oltulelei Tuffs. Clastic dikes of this kind have not been recorded in the OL Fm. strata of Locality G.

Oltepesi (OT) Member

The Oltepesi Member lies between the top of the Oltulelei Tuffs (190 ka) and the base of the Tinga Member megaclastic flood sediments (~50 ka) (Text Fig. 4, Figs. DR3A-DR3C). The thickest deposits are preserved in well-defined valley fills in Localities B, OLT, and G, but this member also includes a wide variety of other lithofacies in Localities C and G.

Phase B-5

In Locality B, the reddish brown, carbonate-rich deposits of the OT Mb. are easily distinguished from underlying white sediments of the OG Fm. and the typical pale yellow to gray sediments of the OK Mb. (Text Figs. 6, 7). The lower OT deposits in Locality B (Phase B-5) fill a drainage network cut into the older strata (Text Figs. 4–7, Fig. DR3A), with multiple valleys converging toward the outflow constriction in the northwest where the present river cuts through Mt. Olorgesailie lavas (orange dashed lines in Text Fig. 6). The deepest parts of the erosional incisions are 11–12 m below the valley tops near the drainage exit through the lavas, decreasing in depth in the paleo-upstream direction toward the east. The basal valley fill deposits are composed of reworked materials from the surrounding terrain, including lava cobbles, blocks of diatomite and carbonate from the OG Fm., and angular clasts of the Oltulelei Tuffs. Above this basal valley fill, the sediments consist of reworked pumice, reddish brown silt and sand, and lithic gravels in varying proportions, poorly sorted, with carbonate rhizoliths, occasional thin paleosols, and localized occurrences of fossil vertebrates and artifacts. Bedding is irregular and discontinuous, with few preserved primary sedimentary structures. There is no evidence for significant channel cutting and filling within the Locality B valley fill (Text Fig. 4, Fig. DR3A). As fluvial processes were undoubtedly involved in filling the valleys, this indicates relatively continuous aggradation. The absence of cross-stratification and other fluvial sedimentary structures suggests overprinting by plant and vertebrate bioturbation, though no clear footprints have been documented. A well-preserved fossil termitery was recorded in the upper part of the valley fill in Section B08–05.

Besides the prominent OT Mb. valley fill deposits in Locality B, isolated outcrops of reddish-brown silts with abundant carbonate rhizoliths rest unconformably on the OK Mb. and likely belong to the OT Mb. Some of these include reworked pumice, but assignment to one of the depositional phases of the Locality B OT Mb. awaits further dating and geochemical analysis.

Phase G-5

Interbedded, pedogenically modified red and green clays, conglomerates, and diatomaceous silts characterize Phase G-5, which is assigned to the OT Mb. based on the presence of tabular coarse conglomerates and an incised channel similar in scale to those in

Localities B and OLT (Text Fig. 4; Fig. DR3C). G-5 is 4.0–7.0 m thick except in the north end of the exposures where it includes 10–11 m of mostly coarse-grained channel fill (Fig. DR3C). The conglomerates are composed of poorly sorted, angular to sub-rounded clasts of basalt and scoria. Based on sedimentary structures and lithology, plus the westward orientation of the incised paleochannel, these are interpreted as alluvial fan deposits from Mt. Olorgesailie that interfinger with finer sediments accumulated in low areas along the faulted western margin of the mountain (Text Figs. 2, 3, Fig. DR3C). One such deposit with large angular boulders floating in a silty matrix appears to be a mudflow (Text Fig. 4, Fig. DR3C - Section G01–01); this marks the local base of the OT Mb. The top of G-5 is a dark gray tuff with white, vertical plant stem casts can be traced for hundreds of meters north to south along the outcrop; this unit is designated as Upper Plant Stem Tuff (UPST) (Text Figs. 4, Fig. DR3C). It includes white, silicified plant stems in growth positions and caps clays and diatomaceous silts indicating laterally extensive wetlands deposition following the filling of the incised channel.

Phase B-6

Up to 3 m of fine, well-sorted, unconsolidated sand with dispersed small pumices and silt clasts occur along the western margin of Locality B and on isolated hills near this margin. These deposits appear to be eolian and are thickest along the ridge formed by the shoulder of Mt. Olorgesailie (Text Figs. 2, 6, DR3A).

Phase OLT-3

In Locality OLT, a unique sequence of deposits occurs along the eastern side of the Olkesiteti River, near the eastern boundary of Locality OLT and the Lava Peninsula fault (Text Fig. 2, Fig. DR3B - Section OLT01–01). This consists of ~5.8 m of silts that transition upward to pumice gravels, diatomaceous silts, and carbonate beds. The basal unit includes reworked clasts from underlying lava basement, overlain by pedogenically modified calcareous silts, irregularly bedded pumice gravels, and diatomaceous silts with laminated carbonate and possible stromatolitic structures. Diatoms identified in the fine-grained silt unit of Section OLT05–01 indicate a shallow fresh water environment (Owen et al., 2014). Lithic grit and pumices occur in varying concentrations throughout. Phase OLT-3 underlies an orange paleosol and deposits of the Tinga Mb. but is lithologically unlike other OT deposits in Locality OLT. The assignment of Phase OLT-3 to the OT Mb. is based on the date of 168 ka for pumice-bearing units in Section OLT01–01, which represent a distinct influx of volcaniclastics subsequent to the widespread Oltulelei Tuffs.

Phase OLT-4

These deposits occur in a valley (11.8 m deep and 70–80 m wide; Text Figs. 4, 5H, Fig. DR3B), similar physiographically to the valley fill in Locality B (Phase B-5), and include light orange to reddish clastic sediments that contrast markedly with the underlying OG Fm. and OK Mb. As in Locality B, basal deposits include reworked blocks of the Oltulelei Tuffs, reworked diatomite from the OG Fm., and lithic cobbles. Above the lower 2 m, however, the valley fill consists of fine-grained silty sands interbedded with a few pumice-bearing units and gravelly sands, in contrast to the poorly sorted, pumice-rich OT Mb. valley fill in Locality B. One of the upper pumice-bearing units has been dated at 103 ka (Text Table 1, Text Fig. 4). No artifacts and only rare vertebrate fossils have been found in these deposits, which also have fewer calcareous rhizoliths and less pedogenic carbonate than OT deposits in Locality B. Also unlike Locality B,

there were several phases of local channel cutting and filling within the OLT-4 valley fill, and one intra-valley channel fill consists of gravelly sands with abundant reworked silicified plant casts. The OLT-4 valley fill is oriented N-S and continues on the south side of the present Ol Keju Nyiro River. We assume that the flow direction was N to S, following the regional slope, which would require a bend toward the west based on inferred regional drainage configuration ultimately feeding into an outlet through the Ol Keju Nyiro gorge (Text Figs. 6, 9E–F).

Phase OLT-5

This unit consists of 4–5 m of OT Mb. fluvial silts and sandy silts continuing and overtopped the OLT-4 valley fill to create a widespread depositional plain. OLT-5 fines upward to a distinctive, laterally extensive red-orange paleosol exposed on both the north (Text Fig. 5H) and south sides of the modern Ol Keju Nyiro River valley. This paleosol represents temporary stabilization of the Oltepesi depositional plain between 103 ka (Text Table 1) and 50 ka (Deino and Potts 1990).

Phase OLT-6

Up to 3.5 m of very well-sorted, light brown fine sands with occasional silty sands and dispersed small pumices overlie the red-orange paleosol that caps Phase OLT-5 (Text Fig. 5H). A thin volcanic tuff at the base of this unit is dated at 50 Ka (Deino and Potts 1990). Fine-scale horizontal lamination, fine grain size, and excellent sorting of this unit indicate eolian deposition. These sediments include fragments of obsidian and other lithics. The thickest deposits of OLT-6 occur in the higher topographic areas, and we interpret these outcrops as remnants of more widespread, poorly consolidated deposits that were removed during high-energy flows associated with the overlying Tinga Member. Boulders from the flood deposits occur on top of the sands, however, so there is little doubt about the sequence of events.

Phase G-6

Phase G-6 consists primarily of beds of coarse conglomerates that form a laterally extensive mantle capping the outcrops along the eastern margin of Locality G (Text Fig. 5E). Lithofacies also include red, pedogenically modified gritty clays and silts, silty sands, and abundant pedogenic carbonate and caliche. One archaeological site has been excavated in a G-6 paleosol. No tuffs or other volcaniclastic units are known in G-6. The coarsening upward of G-5 to G-6 indicates increased influence of alluvial fan deposits derived from the northwestern slopes of Mt. Olorgesailie (Text Figs. 3, 9).

Phase G-7

Approximately 1.2 km west of the Locality G exposures, along the modern Ol Keju Nyiro River channel, a 4.5 m sedimentary sequence includes interbedded diatomaceous silts, pumice gravels, tuffs, and siliciclastic units that bear no obvious resemblance to Locality G sediments or to the older OG Fm. The basal diatomaceous silts overlie eroded basement of Magadi Trachyte (Text Fig. 2), and G-7 sediments extend south in the modern river channel for some 1 km. Phase G-7 sediments are overlain unconformably by 3–4 m of unconsolidated floodplain deposits recently incised by the Ol Keju Nyiro River. The G-7 deposits represent mixed lacustrine, fluvial, and volcaniclastic deposition. They may be equivalent in age to the upper part of G-4 or G-5, but at present the two outcrop areas cannot be correlated based on stratigraphy and lithology.

Phase G-8

About 1.2 km south of G-7 exposures along the Ol Keju Nyiro channel is a 3.6 m sequence of orange silty sands with pumice gravels and interbedded silts that fines upward to weakly laminated, pedogenically modified silts. These sediments resemble lithologies in OT Phase B-5, with rounded, small gray pumices in finer matrix, but lack volcanic lithics and reworked sediment clasts and are generally better sorted than B-5. G-8 sediments appear to occur stratigraphically above G-7 but the boundary is not exposed; they are overlain by floodplain deposits of the recent Ol Keju Nyiro River. G-7 and G-8 exposures are of interest because they are the closest OL Fm. outcrops to the ODP coring sites, ~15 km to the south (Text Fig. 3) (Pennisi, 2013; Potts et al. 2014; Cohen et al., 2016).

Phase C-1

These spatially limited but informative OT Mb. deposits occur in the southwest part of Locality C (Text Figs. 2, 4, 6). They include complex, cross-cutting channels with black to gray pumice gravels above an irregular erosional unconformity on OG Fm. Mbs 8 and 9 (Text Fig. 5I). Sediments also include poorly sorted gravelly sands and silts with abundant silicified plant casts. A section of a fossil palm tree discovered in these deposits in 1987 has been dated at ~93 ka (Text Table 1), based on associated pumice lapilli. Phase C-1 deposits are exposed for ~200 m along the northern margin of the modern Ol Keju Nyiro River. Based on current directions and lithology, they likely represent a major influx of volcaniclastic sediments transported from the north by the proto-Olkesiteti River. The relationship of C-1 to the other OT depositional phases is not clear but may be resolved by future dating and chemical correlations; we currently interpret it as slightly post-dating the OT Phase B-5 valley fill (Text Figs. 4, 9F; Fig. DR3A).

Tinga (TG) Member

Throughout the area north and northeast of Mt. Olorgesailie, many outcrops are capped by distinctive boulder conglomerates, some with individual lava clasts 4- 5 m in maximum diameter. These are associated with pumice conglomerates and tuffaceous sands as well as basal units with reworked clasts from underlying OG and OL Fm. sediments. Isolated large boulders also occur across the landscape (Text Fig. 5K, L) and represent remnants of more continuous TG Mb. deposits that have been removed by erosion. One of these with a diameter of ~4m (13m circumference) was calculated to weigh 35,000 kg (Text Fig. 5L). The presence of these unusual deposits was recognized by Baker and Mitchell (1976; Baker et al., 1988), who interpreted them as resulting from a catastrophic flood event that entered the Olorgesailie basin from the Kedong Depression to the north (Text Fig. 2). Many of the boulders are composed of distinctive porphyritic basalt linking them to a source in the Kedong Gorge (W.G. Melson, Pers. Comm.). Satellite imagery clearly shows the sediment fan from this event that spread across the Oltepesi Plain (Text Figs. 2, 6, 9G–H).

Phase B-7

In Locality B, the flood deposits (Text Figs. 4; Fig. DR3A; Phase B-7) once covered much of the northern part of the area, as indicated by stratified boulder conglomerates capping isolated hill tops, huge individual boulders resting on eroded OG Fm., OK and OT outcrops, and

boulder and tuff-filled channels cut into earlier deposits near the confluence of the Olulelei and Ol Keju Nyiro Rivers. TG Mb. deposits also occur west of Locality B on the north side the Ol Keju Nyiro River, continuing through the southern part of Localities A and D to a west-directed channel cross-section northwest of the Scoriaceous Cone (Text Figs. 3, 9). Typical TG Mb. lithofacies in Locality B are 1.0–2.0 m thick and include clastics reworked from underlying sediments, pumice conglomerates, and gray brown tuffs (e.g., B09–01). TG deposits frequently coarsen upward from tuffs and pumice gravels into matrix- or clast supported boulder conglomerates, indicating that early stages of the flood events brought in more easily mobilized sediment, followed by the transport and deposition of boulders weighing hundreds to tens of thousands of kilograms (Text Fig. 5K, L). There is little doubt that flood events needed to move these clasts required enormous volumes of water and transport energy.

Phase OLT-7

In Locality OLT, TG Mb. deposits (Text Fig. 4, Fig. DR3B; Phase OLT-7) also occur along the present Olkesiteti River, the main conduit for floods from the north through the Kedong Depression and the Enkobirri Gorge (Text Fig. 2). Large boulders occur on both the north and south terraces bounding the present ~15-m-deep Ol Keju Nyiro River valley. This provides clear evidence for the original southern extent of the TG Mb. and also indicates that the modern Ol Keju Nyiro valley in western Locality OLT was formed after the major flood events. Much of the Oltepesi Plain is covered by the TG Mb. deposits (Text Figs. 1–3, 6, 9), evidence that the sediment spread out over this area and then was directed westward by the pre-existing drainage exit through the Ol Keju Nyiro Gorge. Sediments overlying TG Mb. boulder conglomerates, exposed along the Olkesiteti River south of the Magadi Road (Text Fig. 2, Fig. DR3b), are included in the Tinga Mb. These include localized sands and a fine-grained gray tuff, originally sampled by Bye et al. (1987) and now identified as the Menengai Tuff, dated at 35.62 ± 0.26 ka (Blegen et al. 2016).

Phase C-2

In southern Locality C, TG Mb. deposits include boulder conglomerates that cap ridges and hills of eroded OG Fm. strata, isolated large boulders, conglomeratic sheet deposits (Text Fig. 4; Phase C-2), and diatomaceous silts. Along the southern border of Locality C, near the Ol Keju Nyiro channel, a flat floodplain is formed by clast-supported pumice conglomerate and volcanic sand with abundant large boulders, some of which have silicified root casts on their undersurfaces. These deposits are capped by well-sorted diatomaceous silts that document temporary ponding after emplacement of the flood deposits. Given these topographic relationships, we propose that the ridge-capping boulder conglomerates and large isolated boulders represent an earlier major flood event and the topographically lower sheet deposit a later one.

As previously mentioned, there currently are no recognized TG Mb. deposits in Locality G, indicating that the constriction provided by the Ol Keju Nyiro Gorge and the barrier formed by the Scoriaceous Cone blocked the onward transport of the TG boulders. There may have been temporary damming at the gorge by the flood deposits, and after river flow was reestablished it lacked sufficient energy to transport the coarser TG sediments. It is likely, however, that at least some of the water and finer sediments from the floods reached Locality G and the Koora Graben,

raising the possibility of identifying these events in the Koora Graben outcrop or drill core records.

Recent Alluvium

In Locality G, ~4 m of well-stratified, unconsolidated fluvial sediments are exposed along the banks of the Ol Keju Nyiro River, indicating one or more periods of floodplain aggradation prior to the onset of modern river incision. The age of these deposits is under investigation, but they overlie the Locality G OL Fm. and likely represent Holocene to sub-recent deposition in the northern portion of the Koora Graben. There are no TG Mb. conglomerates or volcanic tuffs yet identified in this alluvium.

REFERENCES CITED

- Baker, B.H., and Mitchell, J.G., 1976, Volcanic stratigraphy and geochronology of the Kedong-Olorgesailie area and the evolution of the south Kenya rift valley: Journal of the Geological Society, v. 132, p. 467–484, <https://doi.org/10.1144/gsjgs.132.5.0467>.
- Baker, B.H., Mitchell, J.G., and Williams, L.A.J., 1988, Stratigraphy, geochronology and volcano-tectonic evolution of the Kedong-Naivasha-Kinangop region, Gregory Rift Valley, Kenya: Journal of the Geological Society, v. 145, p. 107–116, <https://doi.org/10.1144/gsjgs.145.1.0107>.
- Blegen, N., Brown, F.H., Jicha, B.R., Binetti, K.M., Faith, J.T., Feraro, J.V., Gathogo, P.N., Richardson, J.L., and Tryon, C.A., 2016, The Menegai Tuff: A 36 ka widespread tephra and its chronological relevance to Late Pleistocene human evolution in East Africa: Quaternary Science Reviews, v. 152, p. 152–168, <https://doi.org/10.1016/j.quascirev.2016.09.020>.
- Brooks, A. S., Yellen, J. E., Potts, R., Behrensmeyer, A. K., Deino, A. L., Leslie, D., Ambrose, S., Ferguson, J., d'Errico, F., Zipkin, A. M., Whittaker, S., Post, J., Veatch, E. G., Foecke, K., and Clark, J., 2018, Long-distance stone transport and pigment use in the earliest Middle Stone Age. *Science* (in press).
- Bye, B.A., Brown, F.H., Cerling, T.E., and McDougall, I., 1987, Increased age estimate for the lower Palaeolithic hominid site at Olorgesailie, Kenya: *Nature*, v. 329, p. 237–239, <https://doi.org/10.1038/329237a0>.
- Cohen, A., Campisano, C., Arrowsmith, R., Behrensmeyer, A.K., Deino, A., Feibel, C., Hill, A., Johnson, R., Kingston, J., Lamb, H., Lowenstein, T., Noren, A., Olago, D., Owen, R.B., Potts, R., Reed, K., Renaud, R., Schabitz, F., Tiercelin, J.-J., Trauth, M.H., Wynn, J., Ivory, S., Brady, K., O'Grady, R., Rodysill, J., Githiri, J., Russell, J., Foerster, V., Dommain, R., Rucina, S., Deocampo, D., Russell, J., Billingsley, A., Beck, C., Dorenbeck, G., Dullo, L., Feary, D., Garello, D., Gromig, R., Johnson, T., Junginger, A., Karanja, M., Kimburi, E., Mbuthia, A., McCartney, T., McNulty, E., Muiruri, V., Nambiro, E., Negash, E.W., Njagi, D., Wilson, J.N., Rabideaux, N., Rabu, T., Sier, M.J., Smith, P., Urban, J., Warren, M., Yadeta, M., Yost, C., and Zinaye, B., 2016, The Hominin Sites and Paleolakes Drilling Project: Inferring the Environmental Context of Human Evolution from Eastern African Rift Lake Deposits: Scientific Drilling, v. 21, p. 1–16, <https://doi.org/10.5194/sd-21-1-2016>.
- Deino, A., and Potts, R., 1990, Single crystal $^{40}\text{Ar}/^{39}\text{Ar}$ dating of the Olorgesailie Formation, southern Kenya rift: *Journal of Geophysical Research*, v. 95, no. B6, p. 8453–8470, <https://doi.org/10.1029/JB095iB06p08453>.

- Deino, A. L., Behrensmeyer, A. K., Brooks, A. S., Yellen, J. E., Sharp, W. D., Potts, R., 2018, Chronology of the Acheulean to Middle Stone Age transition in eastern Africa. *Science* (in press).
- Owen, R.B., Renaut, R.W., Behrensmeyer, A.K., and Potts, R., 2014, Quaternary geochemical stratigraphy of the Kedong-Olorgesailie section of the southern Kenya Rift Valley. *Palaeogeography, Palaeoecology, Palaeoclimatology*, v. 396, p. 194–212. Potts, R., 1994, Variables vs. models of early Pleistocene hominid land use: *Journal of Human Evolution*, v. 27, p. 7–24.
- Pennisi, E., 2013, Out of the Kenyan mud, an ancient climate record: *Science*, v. 341, p. 476–479, <https://doi.org/10.1126/science.341.6145.476>.
- Potts, R., Behrensmeyer, A.K., Deino, A., Kinyanjui, R., Noren, A., 2014, Building the climate context of the Acheulean and Middle Stone Age of East Africa: The Olorgesailie Drilling Project. *PaleoAnthropology PAS abstracts*, A19, 10.4207/PAS.2014.ABS12.

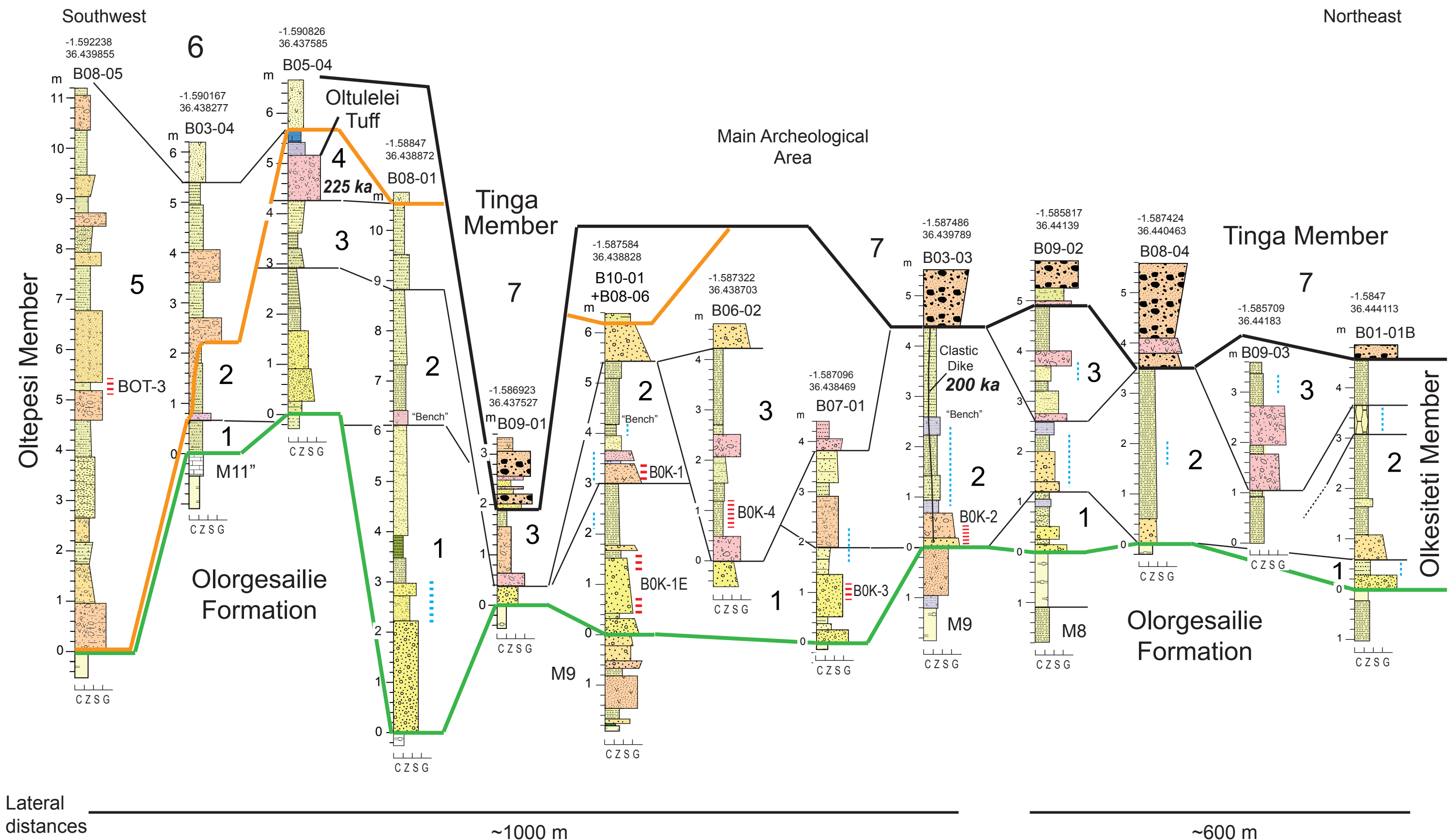
FIGURE CAPTIONS

Figure DR3A. Locality B panel diagram, horizontal distances between sections not to scale. GPS points (Decimal Degrees, WGS84) provided above each section log. Letter and number combinations identify the stratigraphic sections, i.e., B08-05 = Locality B, Year 2008, Section 05, and BOK-1 = Locality B, Archeological Site OK-1. Bold numbers designate depositional phases referred to in text and on Text Figure 4; $^{39}\text{Ar}/^{40}\text{Ar}$ dates in bold italic (see also Text Table 1, DR1, Table DR2). Heavy lines mark the Oltulelei (OL) Fm. Member boundaries: green—base of Olkesiteti (OK) Mb., orange—base of Oltepesi (OT) Mb., black—base of Tinga (TG) Mb. Thinner black lines show lithological correlations and delimit the depositional phases.

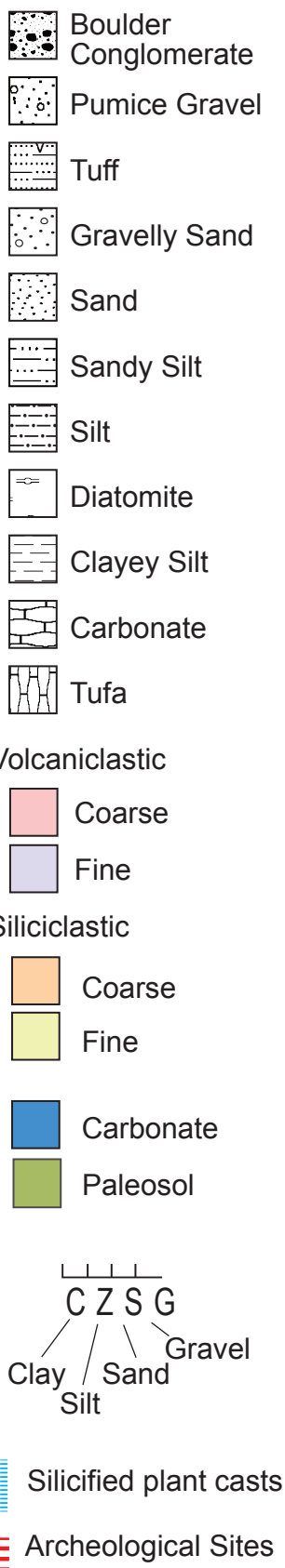
Figure DR3B. Locality OLT panel diagram, horizontal distances between sections not to scale. GPS points (Decimal Degrees, WGS84) provided above each section log. Letter and number combinations identify the stratigraphic sections, i.e., OLT09-01 = Locality OLT, Year 2009, Section 01. Bold numbers designate depositional phases referred to in text and on Figure 4; $^{39}\text{Ar}/^{40}\text{Ar}$ dates in bold italic (see also Text Table 1, Table DR2). Heavy lines mark the Oltulelei (OL) Fm. Member boundaries: green—base of Olkesiteti (OK) Mb., orange—base of Oltepesi (OT) Mb., black—base of Tinga (TG) Mb. Thinner black lines show lithological correlations and delimit the depositional phases.

Figure DR3C. Locality G panel diagram, horizontal distances between sections not to scale. GPS points (Decimal Degrees, WGS84) provided above each section log. Letter and number combinations identify the stratigraphic sections, i.e., G06-05 = Locality G, Year 2006, Section 05, and GOK-1 = Locality G, Archeological Site OK-1. Bold numbers designate depositional phases referred to in text and on Figure 4; $^{39}\text{Ar}/^{40}\text{Ar}$ dates in bold italic (see also Text Table 1, Table DR2). Heavy orange line marks the base of the Oltepesi (OT) Mb (Dashed = inferred position); the base of Olkesiteti (OK) Mb. is not exposed and Tinga (TG) Mb. is not present in Locality G. Thinner black lines show lithological correlations and delimit the depositional phases. “PST” = plant stem tuff.

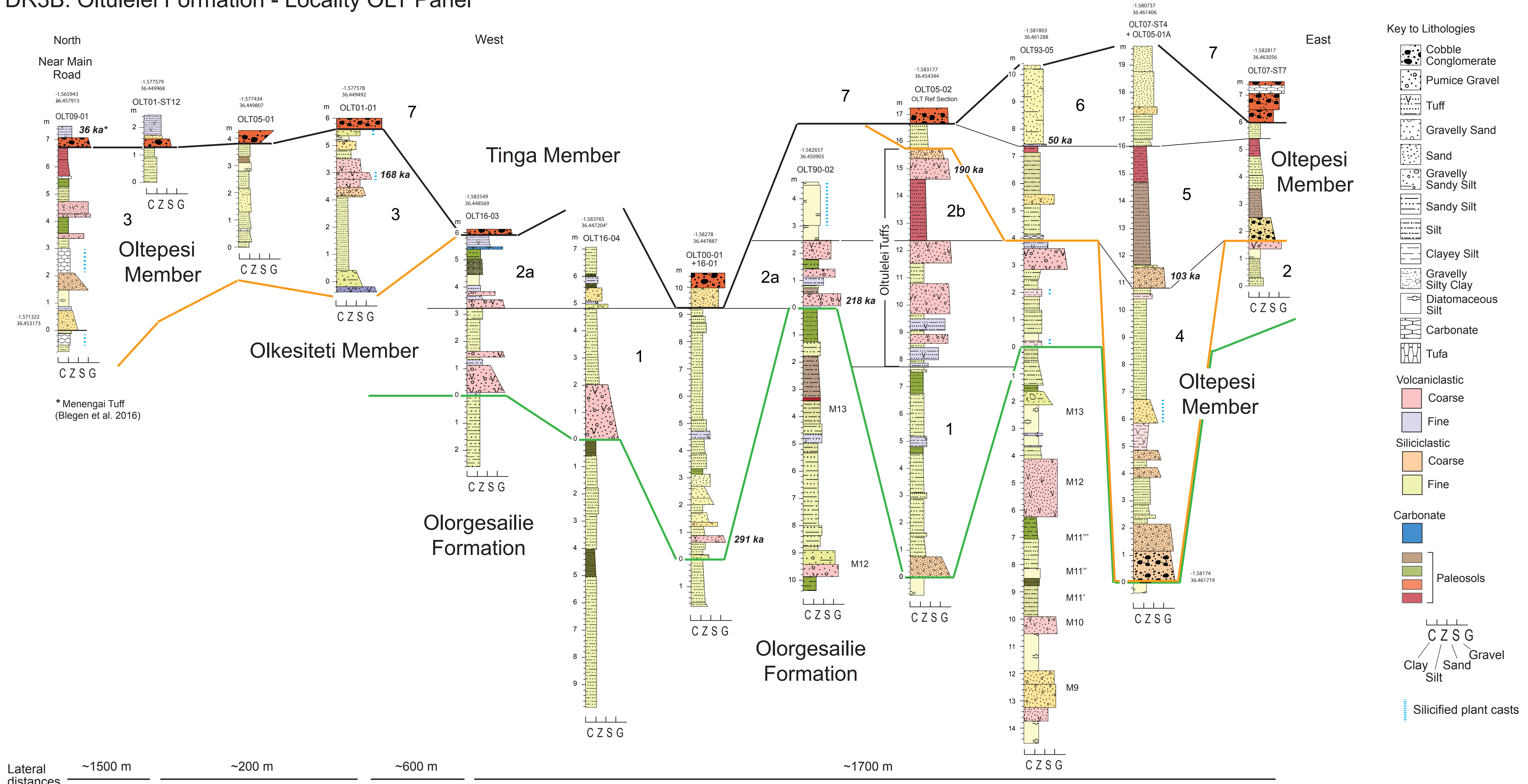
DR3A: Oltulelei Formation - Locality B Panel



Key to Lithologies



DR3B: Oltulelei Formation - Locality OLT Panel



DR3C: Oltulelei Formation - Locality G Panel

